Smurf1 inhibits integrin activation by controlling Kindlin-2 ubiquitination and degradation

Xiaofan Wei,[1]* Xiang Wang,[1]* Jun Zhan,[1] Yuhan Chen,[3] Weigang Fang,[2] Lingqiang Zhang,[3] and Hongquan Zhang[1]

[1]Department of Human Anatomy, Histology, and Embryology, Key Laboratory of Carcinogenesis and Translational Research (Ministry of Education) and State Key Laboratory of Natural and Biomimetic Drugs and [2]Department of Pathology, Peking University Health Science Center, Beijing 100191, China
[3]State Key Laboratory of Proteomics, Beijing Proteome Research Center, Beijing Institute of Radiation Medicine, Beijing 100850, China

Integrin activation is an indispensable step for various integrin-mediated biological functions. Kindlin-2 is known to coactivate integrins with Talin; however, molecules that restrict integrin activation are elusive. Here, we demonstrate that the E3 ubiquitin ligase Smurf1 controls the amount of Kindlin-2 protein in cells and hinders integrin activation. Smurf1 interacts with and promotes Kindlin-2 ubiquitination and degradation. Smurf1 selectively mediates degradation of Kindlin-2 but not Talin, leading to inhibition of αIIbβ3 integrin activation in Chinese hamster ovary cells and β1 integrin activation in fibroblasts. Enhanced activation of β1 integrin was found in Smurf1-knockout mouse embryonic fibroblasts, which correlates with an increase in Kindlin-2 protein levels. Similarly, a reciprocal relationship between Smurf1 and Kindlin-2 protein levels is found in tissues from colon cancer patients, suggesting that Smurf1 mediates Kindlin-2 degradation in vivo. Collectively, we demonstrate that Smurf1 acts as a brake for integrin activation by controlling Kindlin-2 protein levels, a new mechanism that permits precise modulation of integrin-mediated cellular functions.

Introduction

Integrins are transmembrane adhesion receptors that connect cells to the extracellular matrices and mediate bidirectional signaling across the cell membrane (Hynes, 2002). Integrins transduce signals into cells to regulate numerous cellular functions including cell adhesion, spreading, migration, and survival (Legate et al., 2009), thereby contributing to embryonic development and human diseases including cancer (Desgrosellier and Cheresh, 2010). It is well established that Kindlins and Talin are both required for effective activation of integrin (Larjava et al., 2008; Kim et al., 2011; Ye and Petrich, 2011; Ye et al., 2014). Kindlin-2, a member of Kindlin protein family, is widely expressed and evolutionarily conserved (Plow et al., 2009; Lai-Cheong et al., 2010) and is considered a novel and essential regulator for integrin inside-out and outside-in signaling (Montanez et al., 2008; Meves et al., 2009). Loss of Kindlin-2 expression in mice impairs the activation of integrin, resulting in periimplantation lethality. Recent studies show that Kindlin-2 also plays important roles in cancer (An et al., 2010; Yu et al., 2013) and fibrosis (Wei et al., 2013, 2014). Although the functions and importance of Kindlin-2 are well defined, the regulation of Kindlin-2 protein stability is completely unknown.

Ubiquitin-mediated proteasomal degradation is the major pathway that controls the stability and quality of intracellular proteins (Pickart, 2001). E3 ubiquitin ligases play a critical role in this process by recognizing specific substrates. Smurf1, a HECT (homologous to E6AP C terminus) type E3, was originally shown to regulate the bone morphogenetic protein pathway by targeting SMAD1 and SMAD5 (Zhu et al., 1999). Moreover, Smurf1 has been demonstrated to play important roles in multiple biological processes (Zhang et al., 2004; Cao and Zhang, 2013), including embryonic development, cell polarity, cell migration, and bone homeostasis, by promoting the degradation of TGF-βR (Inoue and Imamura, 2008), RhoA (Wang et al., 2003; Sánchez and Barnett, 2012), and MEKK2 (Yamashita et al., 2005). A study showed that Smurf1 mediated Talin-head (Talin-H) ubiquitylation (Huang et al., 2009). Given that integrins play crucial roles in regulating diverse cellular functions, it is interesting and important to investigate whether Smurf1 is involved in the regulation of integrin-related cellular functions.

In the present study, we identified Smurf1 as a novel and important regulator of integrin activation by targeting Kindlin-2, but not Talin, for proteasomal degradation. Smurf1 directly interacts with Kindlin-2 through the WW2 domain of Smurf1 and the PY motif in Kindlin-2. Smurf1 mediates Kindlin-2 polyubiquitination and degradation, leading to impaired activation of integrin. Therefore, Smurf1 exerts a negative impact on integrin-dependent cellular functions including cell spreading, adhesion, and focal adhesion (FA) formation.

*X. Wei and X. Wang contributed equally to this paper.

Correspondence to Hongquan Zhang: hongquan.zhang@bjmu.edu.cn

Abbreviations used: coIP, coimmunoprecipitation; FA, focal adhesion; FN, fibronectin; MEF, mouse embryonic fibroblast; MFI, mean fluorescence intensity; Talin-H, Talin head; Ub, Ubiquitin; WT, wild type.

The Rockefeller University Press $30.00
J. Cell Biol. Vol. 216 No. 5 1455–1471
https://doi.org/10.1083/jcb.201609073

Results

Smurf1 inhibits integrin activation

It has been reported that Smurf1, an E3 ubiquitin ligase that mediates protein degradation, plays an important role in the regulation of cell adhesion and migration, functions that are mediated by integrins (Huang, 2010). We thus hypothesized that Smurf1 may be involved in the regulation of integrin activation. To this end, Flag empty vector or Flag-Smurf1 was transfected into integrin αIIbβ3–expressing CHO cells (CHO-αIIbβ3 cells), a well-described model system for measuring integrin activation (Calderwood et al., 1999; Ma et al., 2006). By measuring PAC1 binding and cell-surface integrin αIIbβ3 expression using flow cytometry, we showed that Smurf1 inhibited the activation of integrin αIIbβ3 by 40% (Fig. 1, A and B). Given that Talin and Kindlin-2 are the two key proteins regulating integrin activation (Ye and Petrich, 2011), we therefore examined the protein levels of Talin and Kindlin-2 under exogenous Smurf1 expression by Western blot analysis. We found that Smurf1 greatly reduced the protein level of Kindlin-2 but did not affect the levels of Talin and the total integrin β3 (Fig. 1 C). Knockdown of Smurf1 by use of three Smurf1 siRNAs increased integrin αIIbβ3 activation, accompanied by up-regulation of the protein levels of Kindlin-2 (Fig. 1, D–F). These findings clearly indicated that Smurf1 regulated integrin activation. It is well known that Talin-H stimulates integrin activation (Calderwood et al., 1999). To answer whether Smurf1 is involved in Talin-H– or Kindlin-2–induced integrin activation, CHO-αIIbβ3 cells were cotransfected with indicated plasmids. As shown in Fig. 1 G, both Talin-H and Kindlin-2 promoted integrin αIIbβ3 activation, with Talin-H displaying a stronger ability to activate integrin than Kindlin-2. Furthermore, coexpression of Kindlin-2 and Talin-H dramatically enhanced αIIbβ3 activation, consistent with the previous study (Ma et al., 2008). In contrast, Smurf1 significantly suppressed Kindlin-2–mediated integrin activation (Fig. 1 G). Moreover, Smurf1 obviously blocked the synergistic effect of Kindlin-2 for Talin-H on integrin activation (Fig. 1 G). Nevertheless, Smurf1 had no impact on Talin-H–triggered integrin activation (Fig. 1 G). In support, Smurf1 remarkably reduced the protein level of Kindlin-2 but did not alter the protein level of Talin-H as measured by Western blot analyses (Fig. 1 H). Furthermore, we demonstrated that Smurf1 inhibited integrin β1 activation in mouse fibroblast NIH3T3 cells by flow cytometry analyses and immunofluorescence using 9EG7 antibody recognizing activated integrin β1 (Fig. S1, A–C). Smurf1 also inhibited Kindlin-2–induced integrin β1 activation in fibroblasts, whereas the E3 ligase inactive mutant (C699A) of Smurf1 could not repress Kindlin-2–induced integrin β1 activation (Fig. 1 I). These data demonstrated that Smurf1 was involved in Kindlin-2–facilitated, but not Talin-H–triggered, integrin activation.

To examine whether the inhibitory effects of Smurf1 on integrin activation and the stability of Kindlin-2 protein are still valid in vivo, mouse embryonic fibroblasts (MEFs) from Smurf1-knockout mice were applied. FACS analyses showed that integrin β1 activation (detected with mAb 9EG7; Byron et al., 2009) were significantly increased in *Smurf1*$^{-/-}$ MEFs (Fig. 1, J and K). Furthermore, rescue of Smurf1 expression in *Smurf1*$^{-/-}$ MEFs inhibited integrin β1 activation. Western analysis showed that depletion of Smurf1 markedly up-regulated the protein level of Kindlin-2 in MEFs, whereas the protein levels of Talin and integrin β1 were not altered by Western blot analyses (Fig. 1 L). Collectively, these findings strongly indicated that Smurf1 is a negative regulator of integrin activation involving control of the protein levels of Kindlin-2, but not Talin and integrin β subunits.

Smurf1 mediates Kindlin-2 proteasomal degradation

Smurf1 is an important E3 ligase, and our results showed that enhanced expression of Smurf1 could reduce Kindlin-2 protein levels and that knockout of Smurf1 reverses Kindlin-2 protein levels. These important facts implied that Kindlin-2 might be a novel substrate of Smurf1. To this end, we scrutinized the function of Smurf1 in mediating the degradation of Kindlin-2. Overexpressed wild-type (WT) Smurf1 in HEK293T cells significantly decreased the protein levels of exogenous Kindlin-2 in a dose-dependent manner (Fig. 2 A). Similarly, Smurf1 reduced the protein levels of endogenous Kindlin-2 (Fig. 2 B). Importantly, the E3 ligase inactive mutant C699A of Smurf1 could not mediate Kindlin-2 degradation (Fig. 2 C). In addition, reduction of Kindlin-2 by Smurf1 was blocked by treatment with MG132, an inhibitor of the proteasome (Fig. 2 D), suggesting that the effect of Smurf1 on Kindlin-2 degradation is mediated by the proteasomal protein degradation pathway. Furthermore, depletion of Smurf1 by two siRNAs in HEK293T cells markedly increased the level of endogenous Kindlin-2 (Fig. 2 E). Consistently, the effect of Smurf1 on Kindlin-2 degradation was also observed in other tumor cell lines, including HeLa, H1299, MCF-7, and MDA-MB-231 cells (Fig. S2).

To investigate whether Smurf1 affects the stability of Kindlin-2 protein, we measured the turnover rate of Kindlin-2 in the presence or absence of Smurf1 using the cycloheximide (CHX) chase assay. Transfection of Smurf1 in HeLa cells led to an obvious reduction in the half-life of exogenously expressed Kindlin-2 compared with the empty vector (Fig. 2 F). Similarly, the half-life of endogenous Kindlin-2 protein was markedly shortened by Smurf1 (Fig. 2 G). Moreover, knockdown of Smurf1 in MDA-MB-231 cells significantly increased endogenous Kindlin-2 stability (Fig. 2 H). These results demonstrated that Smurf1 mediates Kindlin-2 degradation.

Smurf1 promotes polyubiquitination of Kindlin-2

Given that Smurf1 promotes protein degradation, usually through triggering protein ubiquitination (Cao and Zhang, 2013), we thus examined whether Smurf1 mediates Kindlin-2 ubiquitination. To this end, we transfected Flag-Kindlin-2 and HA-ubiquitin expression vectors into HEK293T cells separately with Myc-Smurf1 WT or Myc-Smurf1 C699A, followed by coimmunoprecipitation (coIP) assays. As shown in Fig. 3 A, Kindlin-2 polyubiquitination was greatly enhanced by Smurf1 (lane 3) compared with the control vector (lane 2). Importantly, Smurf1 C699A mutant was unable to promote Kindlin-2 polyubiquitination (lane 4). In vitro, GST-fusion Smurf1 protein expressed and purified from *Escherichia coli* was able to directly mediate strong polyubiquitination on Kindlin-2 (Fig. 3 B). Moreover, knockdown of Smurf1 in MDA-MB-231 cells significantly reduced endogenous ubiquitinated Kindlin-2 (Fig. 3 C). These data suggested that Kindlin-2 can be polyubiquitinated by Smurf1 both in vivo and in vitro.

To pinpoint the possible linkage types of polyubiquitin chains that are linked to Kindlin-2, we applied a series of ubiquitin (Ub) mutant plasmids including Ub-K6R, Ub-K11R,

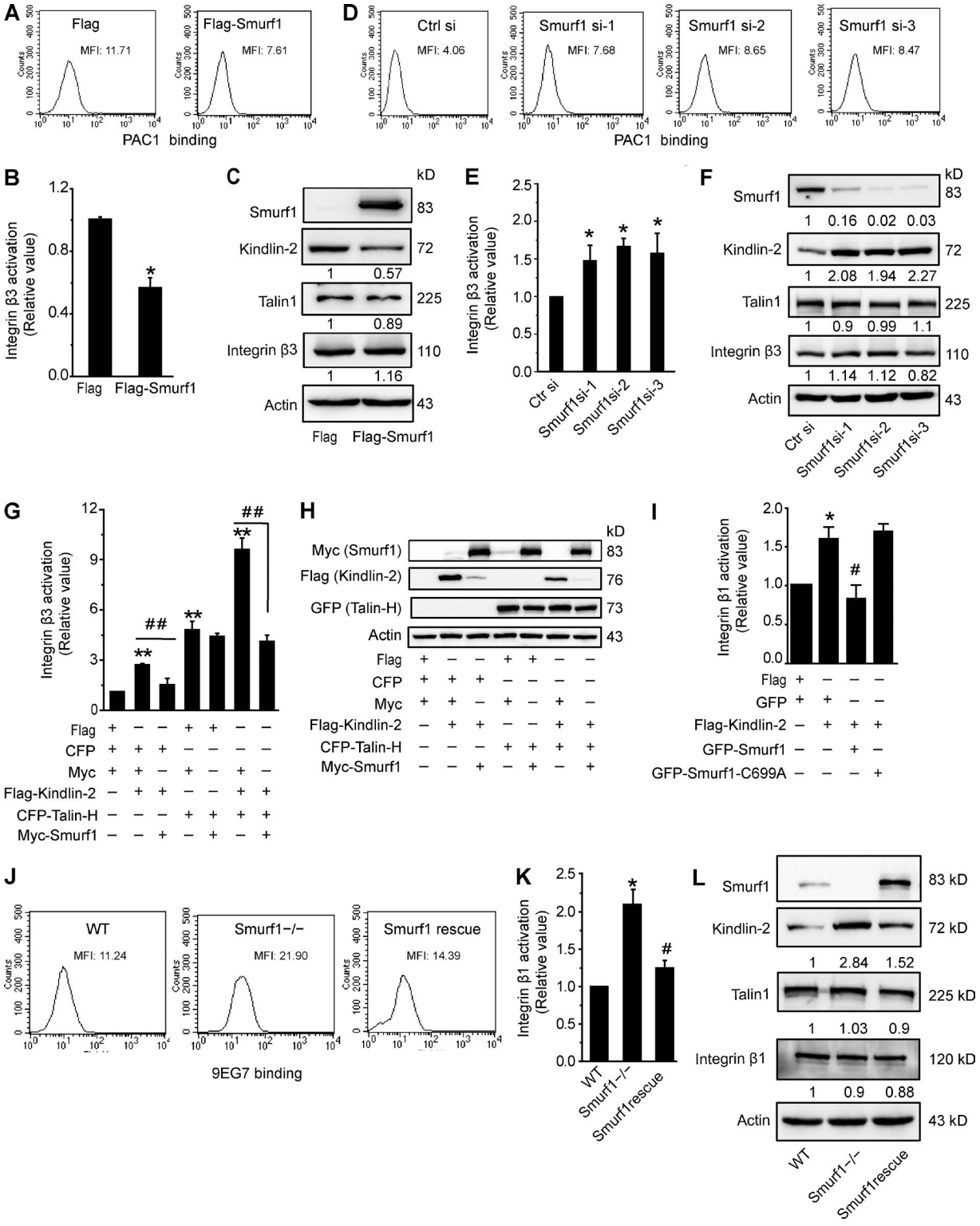

Figure 1. **Smurf1 regulates integrin activation.** (A–C) Flag empty vector or Flag tagged-Smurf1 plasmid was transiently transfected into CHO-αIIbβ3 cells for 48 h. Integrin activation was analyzed using an activation-specific αIIbβ3 mAb PAC1. The values were controlled for cell-surface integrin αIIbβ3 expression levels. Representative FACS histograms of integrin β3 activation are shown (A), and the values were compared with control Flag-expressing cells (normalized to 1). Bars in B represent mean ± SD ($n = 5$). *, $P < 0.05$. (C) Protein expression levels were measured by Western blot with indicated antibodies. (D–F) Control siRNA or Smurf1 siRNA was transfected into CHO-αIIbβ3 cells for 48 h. Integrin activation was analyzed (D and E), and expression levels were measured by Western blot (F). (G and H) CHO-αIIbβ3 cells were transfected with indicated plasmids, and integrin activation was analyzed. The bars in G represent mean ± SD ($n = 5$). **, $P < 0.01$ vs. Flag + CFP + Myc vector group; ##, $P < 0.01$. (H) Expression levels were measured by Western blot with indicated antibodies. (I) Mouse embryo fibroblast cells (NIH3T3) were transfected with indicated plasmids, and integrin activation was analyzed. Bars represent mean ± SD ($n = 5$). *, $P < 0.05$ vs. Flag + GFP vector group; #, $P < 0.05$ vs. GFP + Flag-Kindlin-2. (J and K) β1 integrin activation was detected in *Smurf1*$^{-/-}$, WT, or Smurf1 rescue MEFs using an activation-specific integrin β1 mAb 9EG7. Representative FACS histograms of 9EG7 binding are shown (J). The bars in K represent mean ± SD ($n = 5$). *, $P < 0.05$ vs. WT group; #, $P < 0.05$ vs. Smurf1 KO group. (L) Smurf1, Kindlin-2, Talin, and integrin β1 expression levels were measured by Western blot with indicated antibodies.

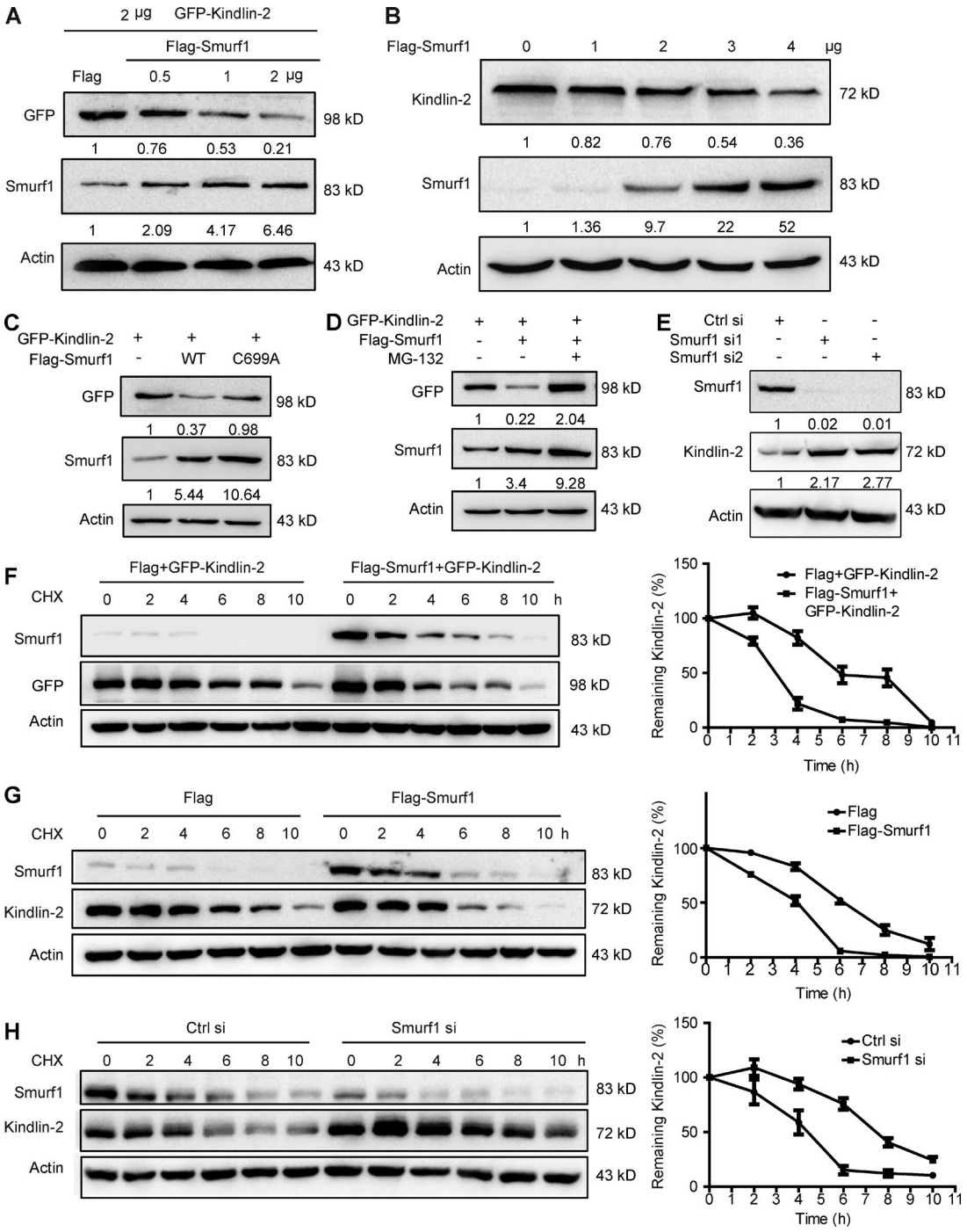

Figure 2. **Smurf1 mediates Kindlin-2 proteasomal degradation.** (A) GFP-Kindlin-2 plasmid (2 μg) was transfected into HEK293T cells together with increasing amounts of Smurf1 WT plasmid. Kindlin-2 expression was determined by immunoblotting with an anti-GFP antibody 24 h after transfection. (B) HEK293T cells were transfected with increasing amounts of Smurf1 expression plasmid, and endogenous protein levels of Kindlin-2 were determined. (C) GFP-Kindlin-2 was transfected into HEK293T cells together with Smurf1 WT or C699A plasmid, and Kindlin-2 expression was examined. (D) HEK293T cells with transfection of GFP-Kindlin-2 and Flag-Smurf1 plasmids were treated with a proteasome inhibitor MG132 (20 μM) or DMSO for 6 h. Kindlin-2 expression was measured. (E) HEK293T cells were transfected with control siRNA or Smurf1 siRNA, and the expression of Kindlin-2 was detected. (F) Flag-Smurf1 was transfected into HeLa cells together with GFP-Kindlin-2, and cells were treated with CHX at 100 μg/ml for the indicated times. The half-life of GFP-Kindlin-2 was measured by Western blot. Quantification of the Kindlin-2 half-life was performed, and each point is represented as the mean ± SD of triplicate experiments. (G) HeLa cells were transfected with Flag-Smurf1, and cells were treated with CHX at 100 μg/ml for the indicated times. The half-life of endogenous Kindlin-2 protein was measured by Western blot and analyzed. Each point represents the mean ± SD of triplicate experiments. (H) CHX-chase experiments of Kindlin-2 in MDA-MB-231 cells transfected with control siRNA or Smurf1 siRNA are shown. Quantification of Kindlin-2 half-life was performed, and each point is represented as the mean ± SD (n = 3).

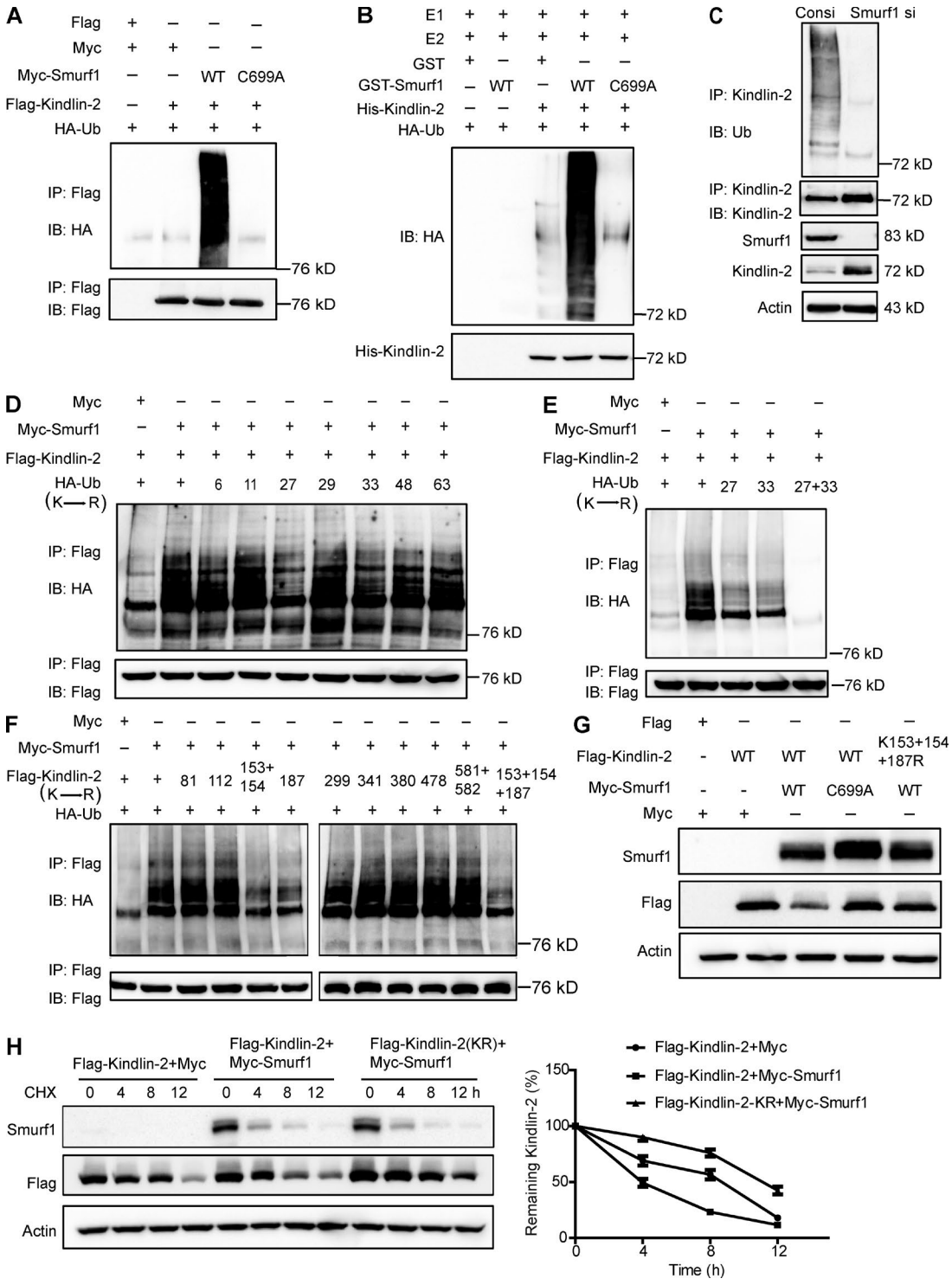

Figure 3. **Smurf1 induces polyubiquitination of Kindlin-2.** (A) Flag-Kindin-2 and HA-Ub were cotransfected into HEK293T cells together with control vector, Myc-Smurf1 (WT), or Myc-Smurf1 (C699A) expression plasmid. Kindlin-2 ubiquitination was detected by immunoprecipitation with anti-Flag M2 beads and immunoblotting with an anti-HA antibody. (B) E1, UbcH5c (E2), HA-Ub, GST-Smurf1 (expressed and purified from bacteria), and His-Kindlin-2 (expressed and purified from bacteria) were incubated at 30°C for 2 h in ubiquitination reaction buffer. Ubiquitinated Kindlin-2 was visualized by immunoblotting with an anti-HA antibody. (C) MDA-MB-231 cells were transfected with indicated siRNAs for 48 h and pretreated with proteasome inhibitor MG132 (10 µM) for 12 h. Polyubiquitination of endogenous Kindlin-2 was detected by anti-ubiquitin antibody. (D) HEK293T cells were transfected with Flag-Kindlin-2, Myc-Smurf1, and various Ub mutant plasmids. 24 h after transfection, an in vivo ubiquitination assay was performed. (E) HA-Ub WT or mutants of K27 and K33 were transfected into HEK293 cells together with Flag-Kindlin-2 and Myc-Smurf1 or control vector. Kindlin-2 ubiquitination was detected. (F) HEK293T cells were transfected with HA-Ub, Myc-Smurf1, and various Kindlin-2 mutant plasmids, and an in vivo ubiquitination assay was performed. (G) HEK293T cells were transfected with Myc-Smurf1 and Kindlin-2 mutant plasmid, and Kindlin-2 levels were assessed. (H) Myc-Smurf1 was transfected into HeLa cells together with Flag-Kindlin-2 WT or Flag-Kindlin-2 K153/154+187R mutant, and cells were treated with 100 µg/ml CHX for the indicated times. The half-life of Flag-Kindlin-2 was measured by Western blot. Quantification of Kindlin-2 half-life was performed, and each point is represented as mean ± SD of triplicate experiments.

Ub-K27R, Ub-K29R, Ub-K33R, Ub-K48R, and Ub-K63R (Kulathu and Komander, 2012). As shown in Fig. 3 (D and E), Ub-K27R and Ub-K33R were found to partially inhibit Smurf1-mediated Kindlin-2 ubiquitination. Importantly, the K27/33R double mutant completely suppressed Smurf1-induced Kindlin-2 ubiquitination. In contrast, other Ub mutants maintained their abilities, as the WT Ub did (Fig. 3, D and E). To scrutinize which sites are responsible for Smurf1-mediated Kindlin-2 ubiquitination, mass spectrometric analysis was performed, and 11 potent ubiquitination sites were identified in Kindlin-2 (Table S1). The 11 Kindlin-2 mutants with K-to-R mutations were generated, and ubiquitination assays were performed in vivo. Among the 11 mutants, K153/154R and K187R were found to be resistant to Smurf1-mediated ubiquitination of Kindlin-2 (Fig. 3 F). Furthermore, as shown in Fig. 3 G, a mutant of Kindlin-2 (K153/154+187R) could not be degraded by Smurf1 compared with WT Kindlin-2 group. The mutation at the Kindlin-2 ubiquitination site significantly prolonged the half-life of Kindlin-2 (Fig. 3 H). These findings suggested that aa residues K153, K154, and K187 of Kindlin-2 are sites that may be linked to ubiquitin. Collectively, these results indicated that Smurf1 mediates Kindlin-2 polyubiquitination via aa residues K27 and K33 of ubiquitin.

Smurf1 does not mediate Talin-H degradation

A previous study showed that Smurf1 mediated Talin-H ubiquitination and degradation (Huang et al., 2009); however, we did not observe that Smurf1 reduces Talin-H protein levels (Fig. 1 H). Because both Talin-H and Kindlin-2 are crucial regulators of integrin activation, we wanted to scrutinize whether Smurf1 mediates Talin-H degradation. To this end, HEK 293T cells were transfected with CFP-Talin-H together with various doses of Flag-Smurf1. Results showed that Talin-H could not be degraded by Smurf1 at different doses (Fig. 4 A). To validate this result, we used the Talin-H-S425A mutant, which is believed to be susceptible to Smurf1-mediated ubiquitination according to a previous study (Huang et al., 2009). However, in this experiment, we did not find that Smurf1 had an obvious effect on Talin-H S425A degradation in HEK 293T cells (Fig. 4 B). To further confirm our results, we then repeated the experiments in other cell lines including HeLa and CHO-K1 cells, which were used in the previous study (Huang et al., 2009). Likewise, Smurf1 was unable to promote degradation of Talin-H or Talin-H S425A in CHO-K1 and HeLa cells (Fig. S3, A–D). Interestingly, we found that MG132 treatment in HEK293T (Fig. 4 C), CHO-K1, and HeLa cells (Fig. S3 E) was unable to increase the protein level of Flag-Talin-H. Given that Smurf1 did not impact the protein levels of full-length Talin (Fig. 1). We further demonstrated that Smurf1 could not interact with full-length Talin, suggesting that Talin is not a target of Smurf1 (Fig. S3 F). These experiments suggested that Smurf1 cannot induce degradation of Talin-H, and Talin-H may be not degraded by the ubiquitin-proteasome pathway.

We next detected whether Smurf1 is able to promote Talin-H ubiquitination. As shown in Fig. 4 D, compared with the control, Smurf1 increased the ubiquitination of Talin-H, whereas Smurf1-C699A mutant abolished the ubiquitination of Talin-H. However, Talin-H ubiquitination by Smurf1 is not a typical polyubiquitination. We demonstrated that Smurf1-induced Talin-H ubiquitination does not act through the K48 linkage type (Fig. 4 E), a major type of ubiquitination that mediates protein degradation. Expression vectors encoding all linkage types of Ub were transfected into HEK 293T cells individually. Results showed that K33 linkage of Ub remarkably increased Talin-H ubiquitination, with intensity similar to that of the WT Ub (Fig. 4 F). The sites responsible for Smurf1-mediated Talin-H ubiquitination were identified by mass spectrometric analysis (Table S2). Ubiquitination assays for Talin-H were performed in vivo using K-to-R mutants K83R, K89R, K98R, and K357R. Results showed that Smurf1 induced Talin-H ubiquitination via aa residues K83 and K357, as indicated by Talin-H mutants K83R and K357R (Fig. S3 G) and a double mutant, Talin-H K83+357R (Fig. 4 G). These results clearly demonstrated that Smurf1 mediates Talin-H ubiquitination but is unable to mediate Talin-H degradation.

Smurf1 interacts with Kindlin-2 in vivo and in vitro

Given that Smurf1 promotes Kindlin-2 polyubiquitination and degradation, we next examined whether Kindlin-2 and Smurf1 physically interact with each other. Flag-Kindlin-2 was transfected into HEK293T cells, followed by coIP with a Flag antibody. As shown in Fig. 5 A, Flag-Kindlin-2 was found to interact with endogenous Smurf1. Furthermore, endogenous Kindlin-2 and Smurf1 showed a strong association in coIP (Fig. 5 B). To test whether this interaction occurs in a direct manner, both full-length His-MBP-Kindlin-2 and GST-Smurf1 proteins were expressed and purified from *E. coli*, and MBP pull-down assays were performed. Results showed that purified Kindlin-2 strongly interacts with purified Smurf1 (Fig. 5 C). To find out whether the interaction between Kindlin-2 and Smurf1 is unique, we further examined the possible interaction of Kindlin-2 with Smurf2. Results showed that Kindlin-2 was unable to associate with Smurf2 in coIP (Fig. 5 D). These data indicated that the interaction between Smurf1 and Kindlin-2 is specific. Moreover, endogenous Kindlin-2 was found to be colocalized with endogenous Smurf1 mainly at focal adhesion sites in HeLa cells by immunofluorescence staining (Fig. 5 E). Collectively, these data demonstrated a previously unknown molecular interaction between Kindlin-2 and Smurf1, both in vivo and in vitro, findings that link together a key focal adhesion molecule and an important E3 ubiquitin ligase.

To map the binding region between Kindlin-2 and Smurf1, three truncated constructs of Smurf1 (Fig. 5 F1) were made. Smurf1 contains a C2 domain at the N terminus, two WW domains in the middle, and a HECT domain at the C terminus. L represents a short linker between the two WW domains of Smurf1. The three truncates were transfected into HEK293T cells, and coIP was performed. Results showed that Smurf1-LW2H domain interacts with Kindlin-2; however, CW1L and HECT domains were unable to interact with Kindlin-2, indicating that Smurf1-WW2 domain interacts with Kindlin-2 (Fig. 5, G and H). Meanwhile, we constructed a series of Kindlin-2 deletion mutants including N-terminal, middle-region, C-terminal, ΔF0, ΔLoop, and ΔPH domains (Fig. 5 F2). As shown in Fig. 5 I, both the N-terminal and FERM domains of Kindlin-2 interacted with Smurf1, and the C-terminal domain of Kindlin-2 was unable to associate with Smurf1 in a GST pull-down assay. In addition, deletion of F0 or PH domains had no effect on the interaction of Kindlin-2 with Smurf1, whereas deletion of the loop region attenuated the interaction (Fig. 5 J). It has been reported that Smurf1 captures its target proteins mainly through the proline-rich (PY) motif in the substrate proteins (Chong et

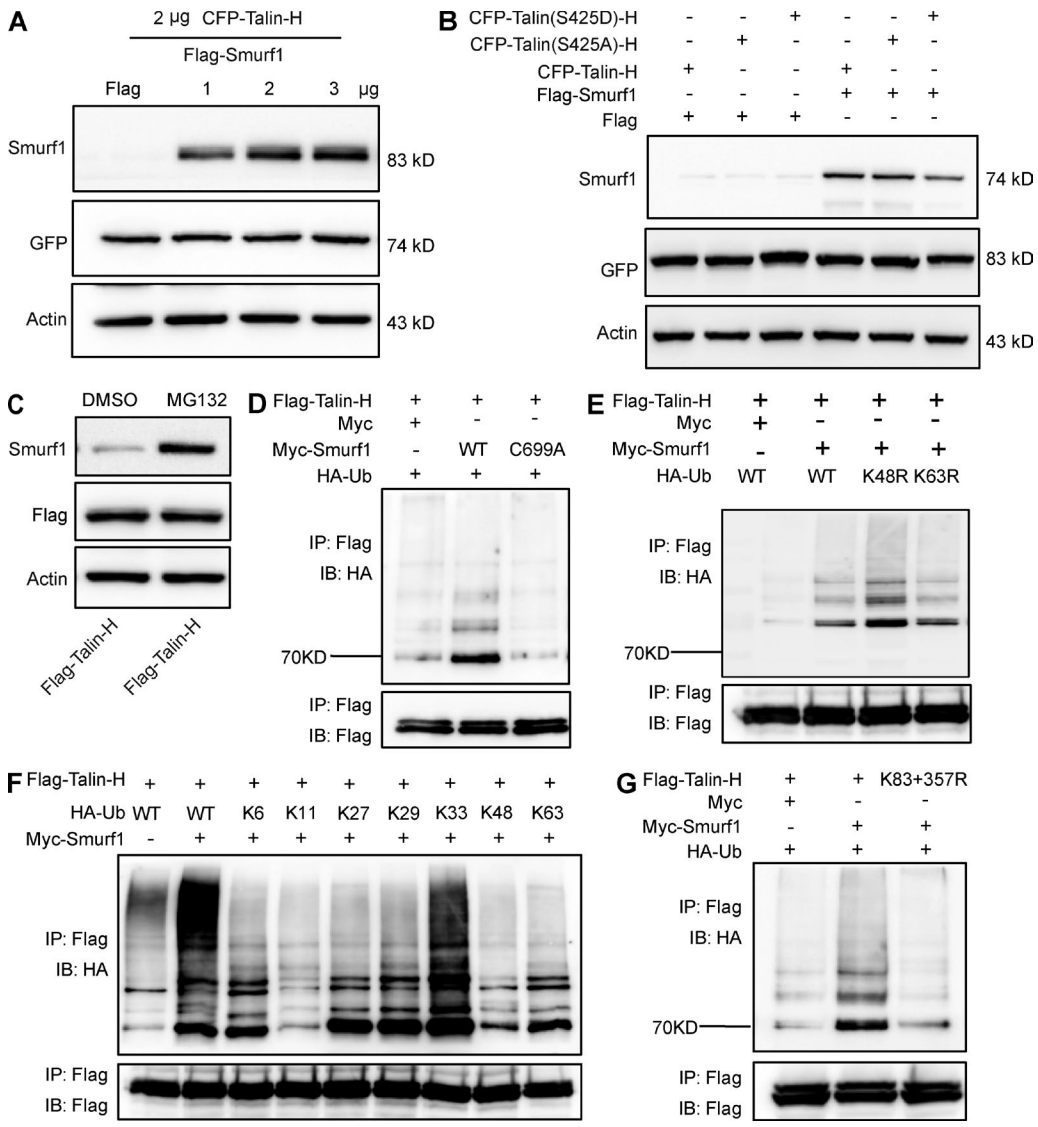

Figure 4. **Smurf1 has no effect on Talin-H degradation.** (A) CFP-Talin-H plasmid (2 μg) was transfected into HEK293T cells together with increasing amounts of Smurf1 expression vector. Talin-H expression was determined by immunoblotting with an anti-GFP antibody 24 h after transfection. (B) Flag-Smurf1 was transfected into HEK293T cells together with Talin-H or mutants of Talin-H, and Talin-H expression was examined. (C) HEK293T cells transfected with Flag-Talin-H were treated with proteasome inhibitor MG132 (20 μM) or DMSO for 6 h, and Smurf1 and Flag-Talin-H protein expression were detected. (D) Flag-Talin-H and HA-Ub plasmids were cotransfected into HEK293T cells together with control vector, Myc-Smurf1 (WT), or Myc-Smurf1 (C699A) expression plasmid. Talin-H ubiquitination was detected by immunoprecipitation with anti-Flag M2 beads and immunoblotting with anti-HA antibody. (E) HEK293T cells were transfected with Flag-Talin-H, Myc-Smurf1, and K48R or K63R Ub mutant plasmids, and after 24 h, an in vivo ubiquitination assay was performed. (F) HEK293T cells were transfected with Flag-Talin-H, Myc-Smurf1, and different linkage Ub plasmids, and after 24 h, an in vivo ubiquitination assay was performed. (G) HEK293T cells were transfected with HA-Ub, Myc-Smurf1, and Flag-Talin-H K83+357 mutant plasmid, and then an in vivo ubiquitination assay was performed.

al., 2010). Interestingly, there is only one PY motif (PGLY) in the loop region of Kindlin-2. To determine whether the PY motif of Kindlin-2 is required for interaction with Smurf1, we mutated the PGLY motif to AGLA. CoIP results revealed that, in contrast to WT Kindlin-2, Kindlin-2 PY motif mutant lost most of its binding capacity with Smurf1 (Fig. 5 K). To validate the importance of the PY motif, ubiquitination and degradation assays were performed using the Kindlin-2 PY motif mutant. Results showed that Kindlin-2 PY motif mutant is protected from Smurf1-induced polyubiquitination and degradation (Fig. S4, A and B). Furthermore, Kindlin-2 PY motif mutant could significantly reverse Smurf1-inhibited integrin activation (Fig. S4 C). These data demonstrated the importance of the PY motif of Kindlin-2 in mediating interaction with Smurf1 and the subsequent cellular functions.

Smurf1 suppresses cell spreading and cell adhesion

The data thus far demonstrated that Smurf1 regulates integrin activation by mediating Kindlin-2 degradation. It is well known that integrin and Kindlin-2 play important roles in the regulation of cell spreading, cell–ECM adhesion, and FA formation. We then wanted to answer whether Smurf1 regulates integrin- and Kindlin-2–related cellular functions. To this end, the spreading dynamics of HeLa cells with overexpression or knockdown of Smurf1 0–120 min after replating on fibronectin

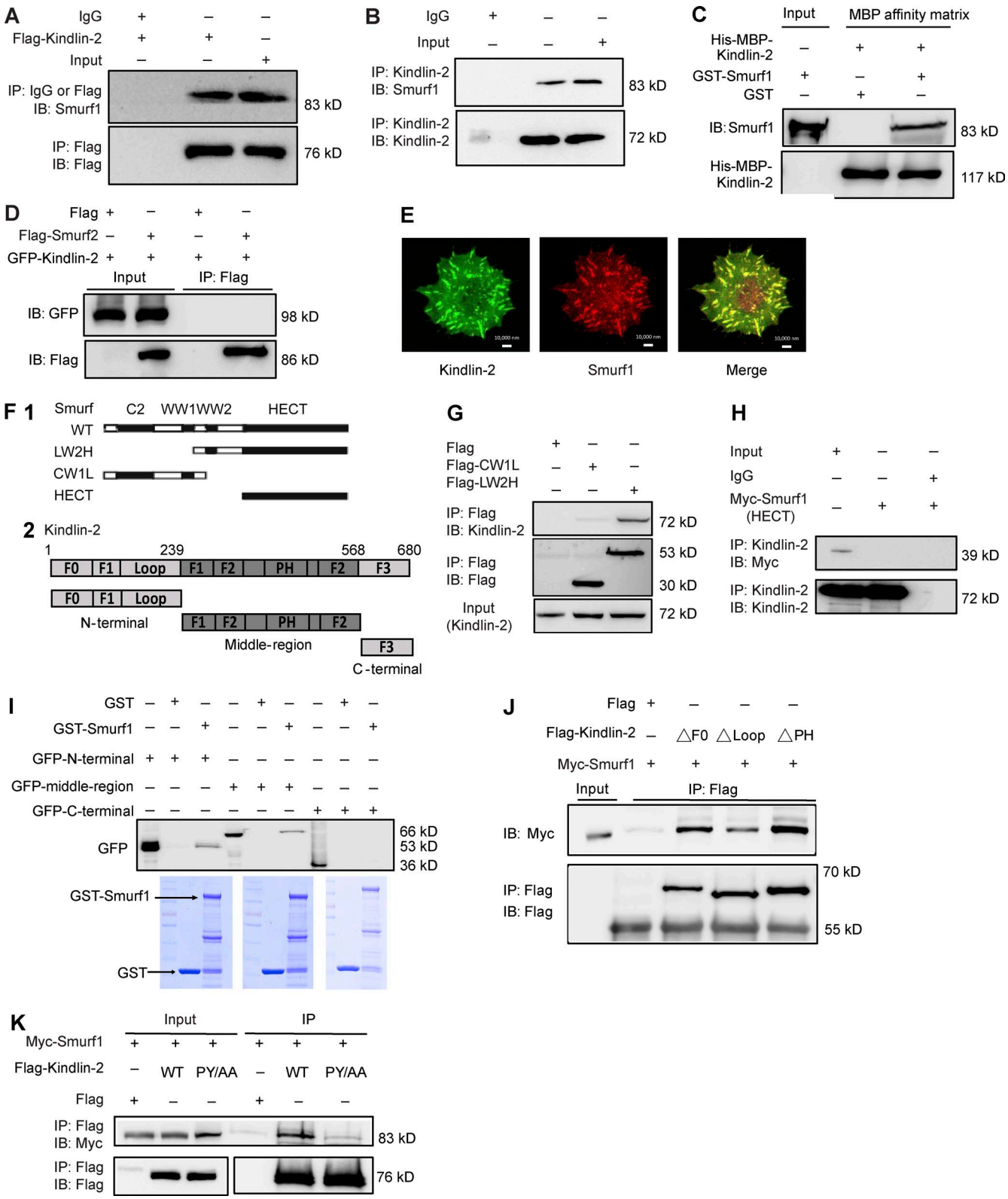

Figure 5. **Smurf1 interacts with Kindlin-2 in vivo and in vitro.** (A) HEK293T cells were transfected with Flag-Kindlin-2. 48 h after transfection, cell lysates were immunoprecipitated with an anti-Flag antibody or normal IgG followed by immunoblotting using Smurf1 antibody. (B) The endogenous interaction between Kindlin-2 and Smurf1 was analyzed by coIP. (C) Fusion protein His-MBP-Kindlin-2 was incubated with GST or GST-Smurf1 in vitro for MBP pull-down assays. Affinity matrices for MBP were used. (D) HEK293T cells were cotransfected with Flag-Smurf2 and GFP-Kindlin-2. 48 h after transfection, cell lysates were immunoprecipitated with anti-Flag antibody followed by immunoblotting using GFP antibody. (E) Colocalization of endogenous Smurf1 and Kindlin-2 was analyzed by immunofluorescence staining. The image was merged. Bars, 10 µm. (F) Indicated truncates of Smurf1 and Kindlin-2 were constructed according to their functional domains. (G and H) HEK293T cells were transfected with the indicated truncates of Smurf1. Cell lysates were immunoprecipitated with anti-Flag antibody (G) or Kindlin-2 antibody (H) followed by immunoblotting using an anti–Kindlin-2 (G) or Myc (H) antibody. (I) HEK293T cells

(FN) were observed under a confocal microscope. Results showed that overexpression or knockdown of Smurf1 significantly inhibited or promoted cell spreading, respectively, from 0 to 60 min, whereas there were no statistical differences between the Smurf1 ectopic expression group and the control group at 120 min, when HeLa cells were fully spread (Fig. 6, A–D). Next, we examined whether these inhibitory effects by Smurf1 were caused by decrease of Kindlin-2 protein levels. Cells were cotransfected with Flag-Kindlin-2 and GFP-Smurf1 (WT or C699A mutant) expression vectors. Compared with the control vector group, Kindlin-2–overexpressing cells spread well, whereas WT Smurf1 notably decreased the percentage of spread cells (Fig. S5, A and B). Smurf1 C699A mutant showed no impact on cell spreading (Fig. S5, A and B). To validate the role of Smurf1 in cell spreading, WT MEFs and *Smurf1*$^{-/-}$ MEFs were applied, and cells were replated on different extracellular matrices including FN, vitronectin, or collagen for cell-spreading assays. Results showed that cell spreading was promoted in *Smurf1*$^{-/-}$ MEFs compared with the WT MEFs. Rescue of Smurf1 expression in *Smurf1*$^{-/-}$ MEFs inhibited cell spreading (Fig. 6, E–G; and Fig. S5, D and E). Similarly, knockdown of Smurf1 promoted cell spreading in HeLa cells (Fig. S5, F and H).

We then determine the role of Smurf1 in cell adhesion. A cell–ECM adhesion assay was performed in HeLa cells with transfection of indicated expression vectors. Results showed that adherent cells were significantly decreased in Smurf1-overexpressing cells (Fig. 6 H). Further, Smurf1 remarkably decreased Kindlin-2–mediated cell adhesion on FN (Fig. 6 H). Consistently, knockdown of Smurf1 increased HeLa cell adhesion on FN (Fig. 6 I). Meanwhile, we found that knockdown of Kindlin-2 significantly inhibited cell adhesion, whereas knockdown of Smurf1 enhanced even stronger adhesive capacity promoted by Kindlin-2, supporting the notion again that Smurf1 mediates Kindlin-2 degradation. More importantly, we found that cell adhesion on FN, vitronectin, and collagen was significantly increased in *Smurf1*$^{-/-}$ MEFs compared with WT MEFs, and reexpression of Smurf1 in *Smurf1*$^{-/-}$ MEFs impaired cell adhesion (Figs. 6 J and S5, J and K). These results indicated that Smurf1 inhibits cell spreading and cell adhesion through mediating the degradation of Kindlin-2.

Smurf1 suppresses FA formation

We continued to investigate whether Smurf1 plays a role in FA formation. For this purpose, HeLa cells were transfected with GFP or GFP-Smurf1 and plated on FN for 60 min, and FA formation was observed under a confocal microscope. Results showed that overexpression of Smurf1 notably decreased the number of FAs/cell and number of FAs/unit area (Fig. 7, A–C). Kindlin-2 is known to promote FA formation, so we examined whether Kindlin-2 degradation is involved in Smurf1-supressed FA formation. Cells were cotransfected with Flag-Kindlin-2 and GFP-Smurf1 (WT or C699A mutant) expression vectors. Compared with the control vector, Kindlin-2–overexpressing cells displayed defined FAs as indicated by robust paxillin staining, whereas WT Smurf1 significantly reduced the number of FAs. Smurf1 C699A mutant showed no impact on FA number (Fig. 7, A–C). Importantly, cells transfected with GFP-Smurf1 and Flag-Kindlin-2 K153/154/187 mutant expression vectors spread well and formed affluent FAs (Fig. 7, A–C). Thus, the Flag-Kindlin-2 K153/154/187 mutant was resistant to ubiquitination by Smurf1 in terms of normal cell spreading and FA formation, supporting the fact that Smurf1 also promotes Kindlin-2 degradation in FAs.

To further demonstrate that Smurf1 has a negative effect on FA formation, WT MEFs and *Smurf1*$^{-/-}$ MEFs were used to detect the number of FAs. In agreement with the earlier findings, FA formation of *Smurf1*$^{-/-}$ MEFs was significantly enhanced compared with the WT MEFs, accompanied by up-regulation of the protein levels of Kindlin-2. Rescue of Smurf1 expression in *Smurf1*$^{-/-}$ MEFs remarkably decreased the number of FAs (Fig. 7, D–F). Similarly, knockdown of Smurf1 promoted cell spreading in HeLa cells (Fig. S5, F and I).

To further investigate the role of Smurf1 in FAs, we measured the rates of adhesion formation and disassembly in protrusive regions of the cell to quantitatively define adhesion turnover parameters. Smurf1 was knocked down in HeLa cells expressing GFP-Zyxin, and GFP-Zyxin was observed from 0 to 15 min, after cells were fully spread (Fig. 7 G). Quantitative analyses showed that knockdown of Smurf1 specifically inhibited the rate of FA disassembly; however, the rate of assembly was not affected (Fig. 7, H and I). Consequently, the mean lifespan of FAs was increased after Smurf1 depletion (Fig. 7 J).

Reverse correlation of Smurf1 with Kindlin-2 in vivo

Although we have demonstrated that Smurf1 mediated Kindlin-2 degradation in a variety of cell lines, it is of importance to know whether this effect also exists under physiological or pathological conditions in vivo. To this end, we examined the amounts of Smurf1 and Kindlin-2 proteins in eight organs obtained from *Smurf1*$^{-/-}$ mice. In Western blot analysis, all the organs except lung showed an obvious increased level of Kindlin-2 protein in *Smurf1*$^{-/-}$ mice compared with WT mice (Fig. 8 A). Results of immunohistochemical staining also showed that expression of Kindlin-2 and Smad1 (a well-known substrate of Smurf1 [Zhu et al., 1999]) was obviously increased in *Smurf1*$^{-/-}$ mouse tissues, e.g., kidney and colon (Fig. 8, B and C). Collectively, these data indicated a negative correlation between Smurf1 and Kindlin-2 in vivo and are probably physiologically relevant.

It was reported that Smurf1 acts as an oncogene in colon cancer (Nie et al., 2014) and that Kindlin-2 functions as a tumor suppressor in colon cancer (Ren et al., 2015). We wanted to examine the protein levels of Smurf1 and Kindlin-2 in colon cancer cell lines. Interestingly, Western blot analysis indicated that Smurf1 protein levels increased in colon cancer cells, with the tumor progression from lower grades to higher ones: SW1116 (Duke's A), LST and SW480 (Duke's B), and SW620 and HCT116 (Duke's C; Fig. 8 D). Intriguingly, Kindlin-2 protein levels decreased with the concomitant increase of Smurf1 protein in the same colon cancer cells (Fig. 8 D). Furthermore, we also found that Smurf1 protein levels are increased in tumor

were transfected with the indicated truncates of GFP-Kindlin-2. Cell lysates were then incubated with GST or GST-Smurf1 in vitro for GST pull-down assays followed by immunoblotting using an anti-GFP antibody. (J) HEK293T cells were transfected with the indicated truncates of Flag-Kindlin-2, and cell lysates were immunoprecipitated with anti-Flag antibody followed by immunoblotting using anti-Myc antibody. (K) The PY motif mutant of Kindlin-2 or Kindlin-2 WT was cotransfected with Smurf1 into HEK293T cells. CoIP was performed with an anti-Flag antibody followed by immunoblotting using an anti-Myc antibody.

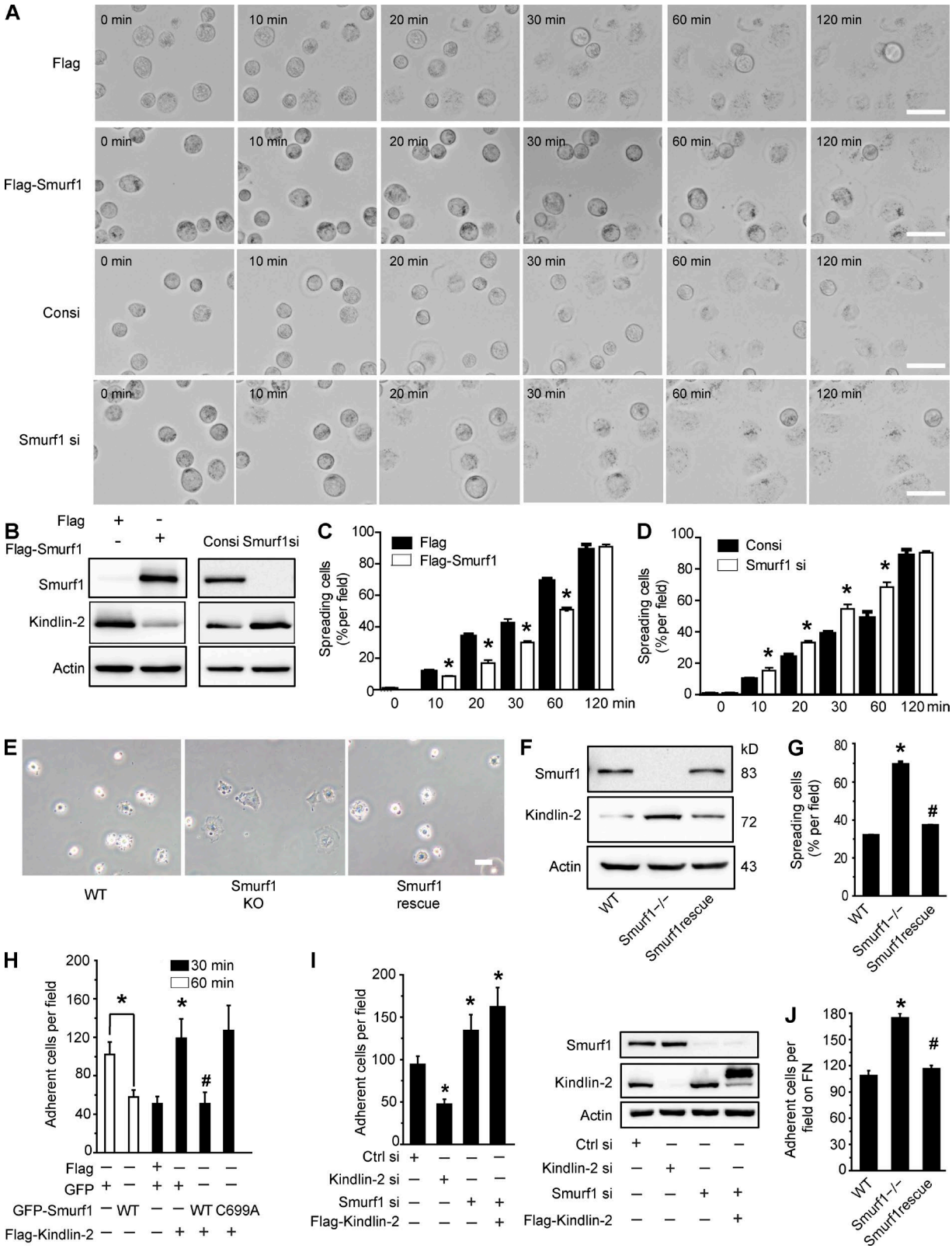

Figure 6. **Smurf1 suppresses cell spreading and adhesion.** (A–D) For dynamic spreading assays, indicated siRNAs or plasmids were transfected into HeLa cells, and the cells were seeded onto 5 µg/ml FN–coated nontreated six-well plates and maintained at 37°C and 5% CO_2 on the microscope stage. Images were collected by a confocal microscopy. Bars, 50 µm. Expression levels of Smurf1 and Kindlin-2 protein were measured by Western blot (B). Flattened and well-spread cells at indicated times were counted. Values are mean ± SD of three independent experiments; *, $P < 0.05$ vs. Flag group (C and D). (E–G) WT, *Smurf1*$^{-/-}$, or Smurf1 rescue MEFs were plated on FN-coated coverslips for 30 min. Spreading phenotypes of cells are shown. Bar, 50 µm. Expression levels of Smurf1 and Kindlin-2 protein were measured by Western blot (F). Graphic presentation of the spreading cells is shown; values are mean ± SD of three independent experiments; *, $P < 0.05$ vs. WT group; #, $P < 0.05$ vs. *Smurf1*$^{-/-}$ group (G). (H) Indicated plasmids were transfected into HeLa cells,

tissues from colon cancer patients compared with normal colon tissues (Fig. 8 E). Meanwhile, Kindlin-2 proteins in corresponding tumor tissues were decreased (Fig. 8 E). Collectively, these results suggested that Smurf1 might control Kindlin-2 degradation in vivo in both physiological and pathological conditions.

Discussion

Integrins function in the regulation of a variety of important biological functions and are linked to many human diseases, including cancer (Margadant and Sonnenberg, 2010). It is well established that both Talin and Kindlins are essential integrin regulators. In this study, we demonstrated that Smurf1, the HECT domain-type E3 ubiquitin ligase, regulates integrin activation by mediating the ubiquitination and degradation of integrin-interacting molecule Kindlin-2, but not Talin (Fig. 8 F). Our findings provide insights into the new functions of Smurf1 and also uncover a novel mechanism underlying the modulation of integrin activation, by controlling Kindlin-2 protein degradation in the integrin-containing focal adhesive structures.

One highlight of this study is that Smurf1 regulates integrin activation. Smurf1 was reported to regulate cell adhesion and migration through ubiquitination of RhoA (Wang et al., 2003) and hPEM2 (Yamaguchi et al., 2008). However, these investigations did not link Smurf1 to integrins and integrin activation. Our finding here directly linked Smurf1 to the activation of integrins through controlling the amount of integrin-interacting FA molecule Kindlin-2. Our results demonstrated that Smurf1 inhibited integrin αIIbβ3 activation in CHO cells and integrin β1 activation in mouse fibroblast NIH3T3 cells. Importantly, integrin β1 activation was significantly increased in *Smurf1*$^{-/-}$ cells. In these processes, Kindlin-2 expression was significantly altered as the Smurf1 protein level changed, whereas the level of the important integrin activator Talin remained unaffected. It was reported that Talin-H is degraded through Smurf1-mediated ubiquitination (Huang et al., 2009), in which Smurf1-mediated Talin-H degradation was examined by only one method, and only ∼30% of Talin-H was degraded by Smurf1. Talin-H was known to play a critical role in integrin activation. Therefore, we assumed that Smurf1 may inhibit integrin activation through promoting Talin degradation. To our surprise, we demonstrated that Smurf1 did not affect integrin αIIbβ3 activation induced by Talin-H alone in CHO-αIIbβ3 cells. Furthermore, we did not observe an obvious effect of Smurf1 on Talin-H degradation in various cell lines. Although Smurf1 had no effects on Talin degradation and integrin activation induced by Talin alone in vitro, Smurf1 does impact integrin activation by controlling the amount of Kindlin-2. This notion suggests an important subtle regulation of the cooperation between Kindlin-2 and Talin in the control of integrin activation under physiological conditions. Collectively, our findings demonstrate for the first time that Smurf1 adds a new layer for limiting integrin activation to fit complicated biological functions.

Several lines of evidence from our present study support the notion that Kindlin-2 is a previously unrecognized substrate of Smurf1. First, Smurf1 directly interacted with Kindlin-2, mainly through the WW2 domain of Smurf1 and the PY motif in Kindlin-2. It is well known that the WW domains of Smurf1 are usually responsible for substrate recognition and PY motif in the substrate proteins that bind to Smurf1. Second, Smurf1 significantly promoted Kindlin-2 degradation in a proteasome-dependent manner. Third, Smurf1 affected Kindlin-2 protein levels by decreasing its stability and shortened its half-life. Fourth, Smurf1 mediated K27- and K33-linked polyubiquitination of Kindlin-2; however, Lys48-linked polyubiquitin in protein degradation is the most common paradigm. Interestingly, Smurf1-mediated polyubiquitination of Kindlin-2 was not through these conventional types but through atypical chain types linked via K27 and K33 (Kulathu and Komander, 2012). Of note, these types of linkage have not been discovered for Smurf1 before. For physiological and disease correlation, the negative correlation of Smurf1 and Kindlin-2 was found in many important organs of *Smurf1*$^{-/-}$ mice and in tumor tissues from colon cancer patients. Identifying new substrates of Smurf1 is an important step for understanding the mechanisms underlying Smurf1-mediated complicated biological processes. Kindlin-2, as a novel substrate of Smurf1, makes Smurf1 function versatile.

In our study, we found that full-length Talin and Talin-H are not targets of Smurf1. Smurf1 could not interact with and mediate the degradation of full-length Talin. Smurf1 also has no effect on Talin-H degradation in various cell lines, despite the fact that Smurf1 does mediate Talin-H ubiquitination. Although ubiquitination is the major way of mediating protein degradation, many ubiquitinated proteins do not use the degradation pathway (Kulathu and Komander, 2012). Types of ubiquitin chain that link to the target protein should be considered, because they may functionally distinct. The role of Lys48-linked chains in proteasomal degradation has been well established; however, other Lys-linked chains may not be involved in protein degradation (Ikeda and Dikic, 2008). We demonstrated that Smurf1 induced Talin-H ubiquitination through ubiquitin K33 linkage. It was reported that ubiquitin-K33 may not mediate protein degradation (Al-Hakim et al., 2008; Huang et al., 2010). Therefore, it is possible that Talin-H could not be degraded by Smurf1 because it is ubiquitinated via ubiquitin K33 linkage. The mechanism underlying degradation of Talin-H or Talin full-length protein remains an interesting open question and warrants future investigations.

We demonstrated functionally that Smurf1 alone inhibited cell spreading, affecting FA dynamics and cell–ECM adhesion with concomitant decrease of Kindlin-2. As expected, Smurf1 significantly suppressed Kindlin-2–induced cell spreading, adhesion, and FA formation. These results are in agreement with the results of the integrin activation assay. Multiple functions of Smurf1 have been discovered in cell growth and morphogenesis, cell polarity, and autophagy by controlling the stability of several important proteins related to embryonic development (Zhu et al., 1999), bone formation (Yamashita et al., 2005), and

the cells were plated on FN-coated coverslips, and attachment of the cells on FN was analyzed at 30 or 60 min from three independent experiments. Values are mean ± SD of three independent experiments; *, P < 0.05 vs. GFP group; #, P < 0.05 vs. GFP + Flag-Kindlin-2 group. (I) Attachment of HeLa cells transfected with control siRNA, Kindlin-2 siRNA, or Smurf1 siRNA on FN was analyzed. Values are mean ± SD of three independent experiments; *, P < 0.05 vs. control group. (J) WT, *Smurf1*$^{-/-}$, or KO rescue MEFs were plated on FN-coated coverslips, and attachment of the cells on FN was analyzed at 30 min. Values are mean ± SD of three independent experiments; *, P < 0.05 vs. WT group; #, P < 0.05 vs. *Smurf1*$^{-/-}$ group.

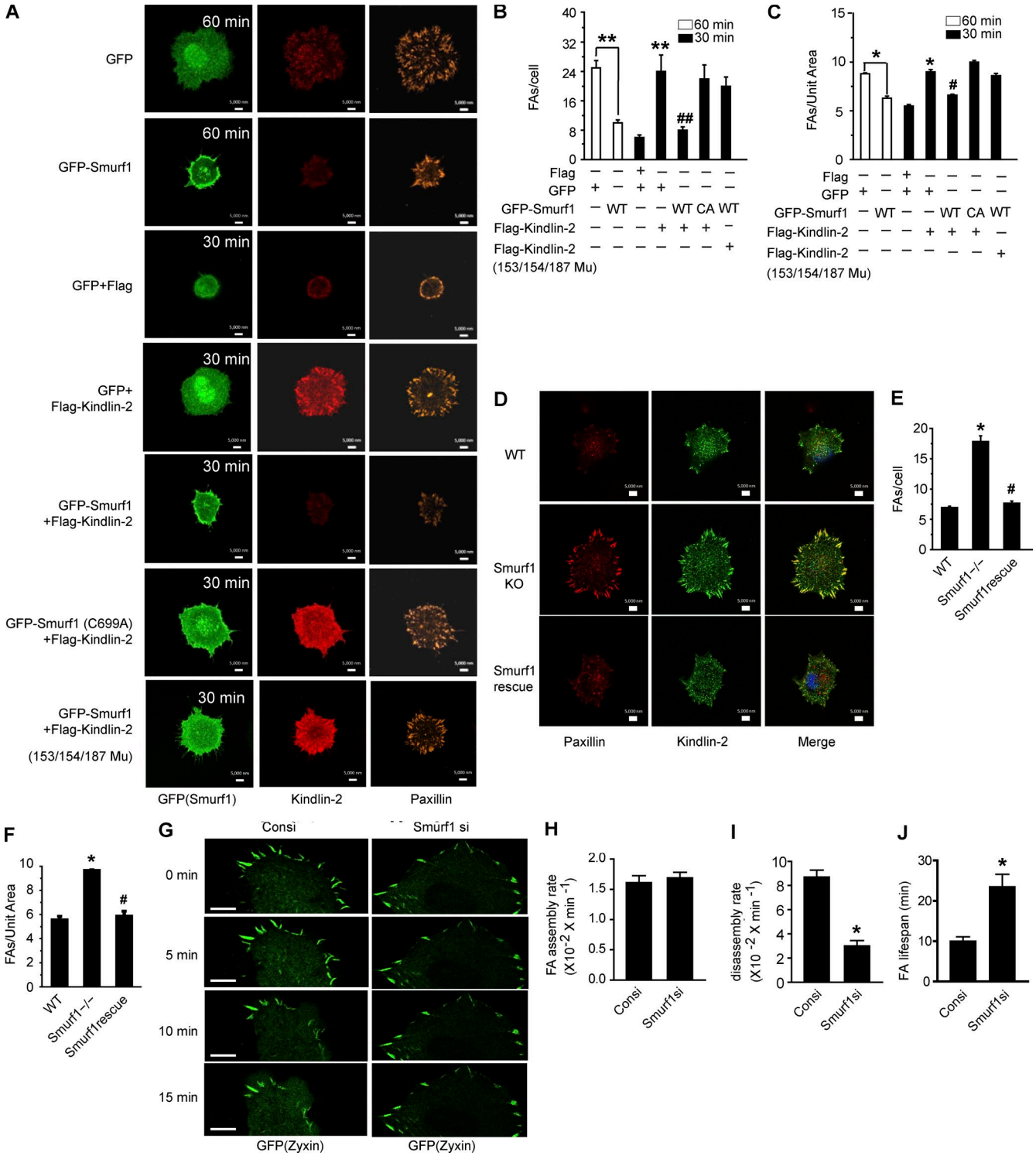

Figure 7. **Smurf1 inhibits focal adhesion formation.** (A) Indicated plasmids were transfected into HeLa cells, then the cells were plated on FN-coated coverslips for 30 or 60 min and immunoreacted with anti-Paxillin and anti–Kindlin-2 or Flag antibodies. Expression and localization of GFP-Smurf1, Kindlin-2, and paxillin were observed under a confocal microscope with 63× objective. Bars, 5 µm. (B and C) Numbers of paxillin-staining focal adhesions per cell (B) and unit area (C) were quantified. Values are mean ± SD of three independent experiments. **, P < 0.01 vs. GFP + Flag group; ##, P < 0.01 vs. GFP + Flag-Kindlin-2 group. *, P < 0.05 vs. GFP + Flag group; #, P < 0.05 vs. GFP + Flag-Kindlin-2 group. Smurf1CA, Smurf1 C699A. (D–F) WT, *Smurf1*$^{-/-}$, or Smurf1 rescue MEFs were plated on FN-coated coverslips for 30 min and immunoreacted with antibody to Kindlin-2 and Paxillin. Expression of Kindlin-2 and Paxillin was determined by confocal microscopy under 63× objective. Bars, 5 µm. Numbers of paxillin-staining focal adhesions per cell and unit area were quantified (E and F). Values are mean ± SD of three independent experiments. *, P < 0.05 vs. WT group; #, P < 0.05 vs. Smurf1 KO group. (G–J) HeLa cells expressing EGFP-Zyxin were transfected with control siRNA or Smurf1 siRNA, plated on FN until fully spread (5 µg/ml), and then analyzed using time-lapse confocal microscopy with 100× objective. Bars, 10 µm. (G) Rate (per minute) of assembly (H), disassembly (I), and lifespan (J) of FAs as measured by change in GFP fluorescence over time for control siRNA and Smurf1 siRNA cells. Values are mean ± SD of three independent experiments; *, P < 0.05 vs. control group.

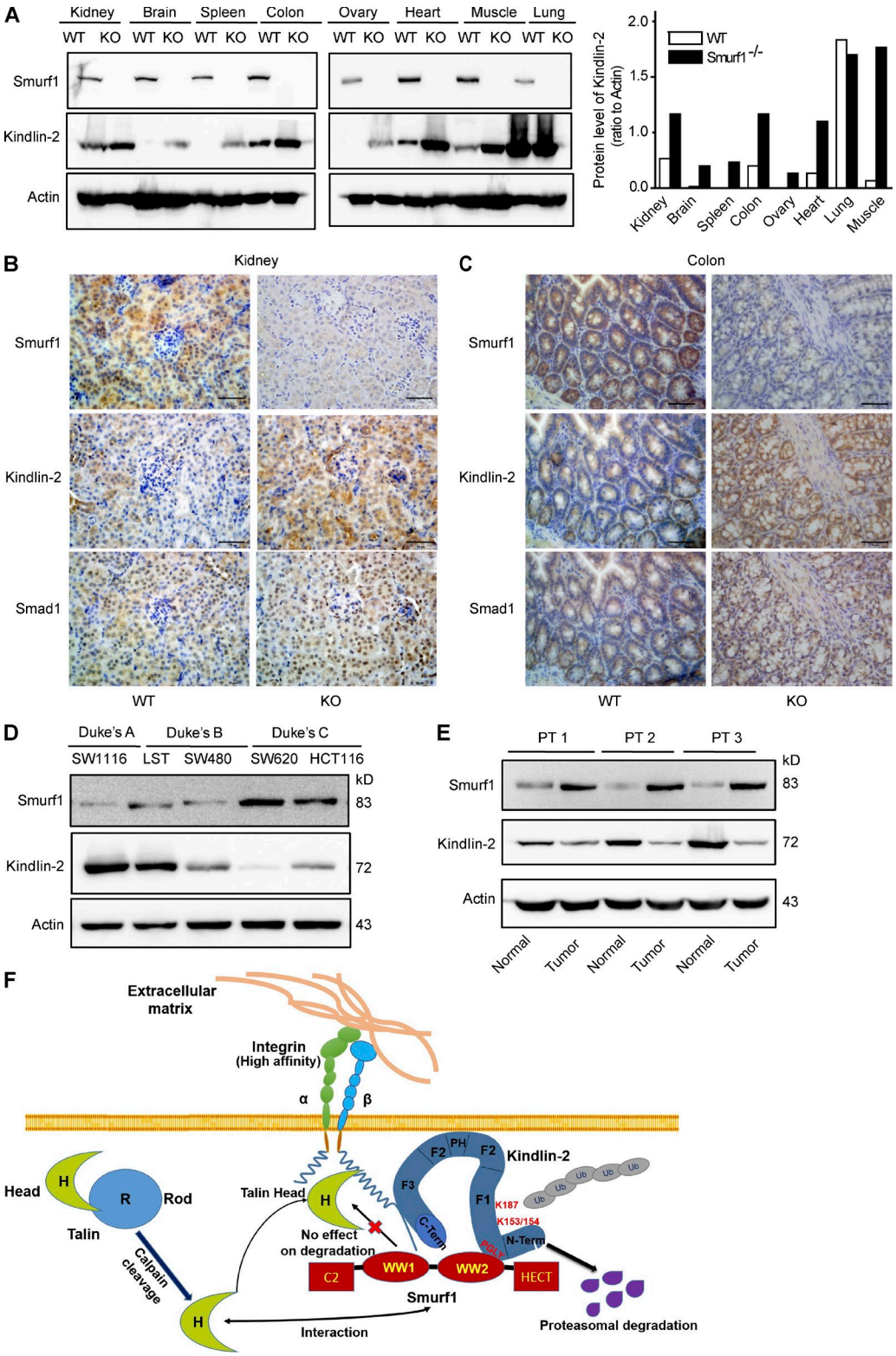

Figure 8. **The expression of Smurf1 is negatively related with Kindlin-2 expression in vivo.** (A) Endogenous Smurf1 and Kindlin-2 protein expression was detected in indicated organs tissues of WT or *Smurf1*$^{-/-}$ mice by Western blot. (B and C) Representative immunohistochemical micrographs showing the expression of Smurf1, Kindlin-2, and Smad1 in the kidney and colon tissues of WT, Smurf1, or *Smurf1*$^{-/-}$ mice. Bars, 50 µm. (D) Smurf1 and Kindlin-2 protein expression in diverse colon cancer cell lines examined by immunoblotting. (E) Smurf1 and Kindlin-2 protein expression in three human colon cancer tissues was determined by Western blot. (F) A hypothetical model for Smurf1 modulation of integrin activation. Both Talin and Kindlin-2 stimulate integrin activation via Talin-H and Kindlin-2 FERM domain binding to integrin β cytoplasmic tail. Smurf1 directly interacts with Kindlin-2 through the Smurf1-WW2 domain and the PY-motif in Kindlin-2. Smurf1 mediates Kindlin-2 polyubiquitination, leading to the proteasomal degradation of Kindlin-2, thereby inhibiting integrin activation. Although Smurf1 interacts with Talin-head, Smurf1 does not mediate the degradation of Talin-H or the full-length Talin. Therefore, Smurf1 does not influence integrin activation mediated by Talin alone. Collectively, Smurf1 controls proper integrin activation by interacting with and limiting the amount of Kindlin-2, a helper in Talin-mediated integrin activation.

cancer progression (David et al., 2013). However, a significant phenotype of Smurf1-knockout mice was observed only in the skeletal system, which showed increased bone mass and enhanced osteoblast activity in Smurf1-deficient mice (Yamashita et al., 2005). Another study found that overexpressed Smurf1 in chondrocytes significantly reduced endochondral ossification (Horiki et al., 2004). Recently, an interesting study (Wu et al., 2015) demonstrated that Kindlin-2 expression is critical for endochondral ossification. Loss of Kindlin-2 impairs formation of the primary ossification center of the long bones and leads to low bone mass (Wu et al., 2015). It is presumable and believable that the regulation of Smurf1 on Kindlin-2 levels may play an important role in skeletal development. Therefore, Smurf1 and Kindlin-2 may be two good targets for bone-related diseases and need to be further investigated. In addition, reverse correlation of Smurf1 and Kindlin-2 was also identified in colon cancer in the present investigation, which is reinforced by studies demonstrating that Smurf1 promotes, whereas Kindlin-2 inhibits, colon cancer progression (Nie et al., 2014; Ren et al., 2015).

In summary, we identified a novel role of Smurf1 by demonstrating that Smurf1 mediates the ubiquitination and proteasomal degradation of Kindlin-2, a coactivator of integrin activation. Smurf1 thereby functions as a brake for restricting integrin activation through controlling the amount of Kindlin-2, which counteracts those that activate integrins. Therefore, by controlling Kindlin-2 protein levels, Smurf1 may play important roles in multiple biological processes and pathophysiological functions.

Materials and methods

Plasmids

The construction of plasmid pFlag-Kindlin-2 and deletion mutants of Kindlin-2 has been previously reported (Wei et al., 2013). To generate Flag-Talin-H (1–433 aa) and CFP-Talin-H, DNA fragments encoding residues 1–433 of Talin were amplified by PCR and inserted into p3×Flag-CMV-10 vector (Sigma-Aldrich) and pECFP-C3 vector. To generate GFP-Kindlin-2, cDNA encoding full-length Kindlin-2 was amplified by PCR and inserted into pEGFP-C3 vector. All constructs were confirmed by DNA sequencing. Myc-Smurf1 WT, Myc-Smurf1-C699A, Flag-Smurf1, Flag-Smurf1-C699A, GFP-Smurf1, truncates of Smurf1, and HA-Ub were described previously (Lu et al., 2008). Point mutations of Kindlin-2 and Ub were generated using a Muta-direct mutagenesis kit (SBS; Genentech). All mutations were confirmed by DNA sequencing.

Antibodies and reagents

The following primary antibodies were used at indicated concentrations for Western blot (WB), immunofluorescence (IF), or FACS: mouse anti-Smurf1 (clone 1D7; ab117552; Abcam), WB, 1:1,000; IF, 1:100; mouse anti-Talin (clone 8D4; sc-59881; Santa Cruz Biotechnology, Inc.), WB, 1:1,000; rabbit anti-paxillin (clone Y113; ab32084; Abcam), WB, 1:5,000; IF, 1:200; rabbit anti–β1 integrin (clone EPR1040Y; ab134179; Abcam), WB, 1:500; FACS, 1:100; rat anti–β1 integrin (clone KMI6; ab95623; Abcam), WB, 1:1,000; FACS, 1:200; mouse anti–β3 integrin (clone VI-PL2; ab110131; Abcam), WB, 1:1,000; FACS, 1:200; rabbit anti–Kindlin-2 (K3269; Sigma-Aldrich), WB, 1:1,000; mouse anti-Flag (clone M2; Sigma-Aldrich), WB, 1:2,000; mouse anti-GFP (clone GSN149; G1546; Sigma-Aldrich), WB, 1:2,000; rabbit anti-Myc (SAB4301136; Sigma-Aldrich), WB, 1:2,000; mouse anti-HA (clone HA-7; H9658; Sigma-Aldrich), WB, 1:5,000; mouse anti–Kindlin-2 (clone 3A3; Mab2617; EMD Millipore), WB, 1:1,000; IF, 1:200; goat anti–Kindlin-2 (clone Y-15; sc-30854; Santa Cruz Biotechnology, Inc.), IF, 1:100; rabbit anti-ubiquitin (3933; Cell Signaling Technology), WB, 1:1,000; rat anti–active-integrin β1 9EG7 (clone 9EG7; 553715; BD), IF, 1:200; FACS, 1:200; ligand-mimetic anti–integrin aIIbβ3 mAb PAC-1 (340507; BD); and mouse anti-actin (clone 2Q1055; sc-58673; Santa Cruz Biotechnology, Inc.), WB, 1:2,000. Secondary antibodies were goat anti–mouse HRP and goat anti–rabbit HRP (both Santa Cruz Biotechnology, Inc.), WB, 1:5,000; donkey anti-mouse Alexa Fluor 488 (A21202); donkey anti-rabbit Alexa Fluor 488 (A21206); donkey anti-goat Alexa Fluor 488 (A11055); donkey anti-mouse Alexa Fluor 568 (A10037); donkey anti-rabbit Alexa Fluor 568 (A10042); goat anti–mouse Alexa Fluor 633 (A21126); goat anti–rat IgM Alexa Fluor 647 (A21248; all Invitrogen), FACS, 1:300; IF, 1:400. Proteasome inhibitor MG132 (SML1135) and protein synthesis inhibitor cycloheximide (C7698) were purchased from Sigma-Aldrich.

Cell culture and transfection

MEFs were isolated from embryonic day 12.5 (E12.5) embryos and cultured in DMEM supplemented with 10% FBS, penicillin/streptomycin, and 2 mM L-glutamine using standard techniques. Human embryonic kidney (HEK293T), CHO-K1, and human cervical carcinoma (HeLa) cells were cultured in DMEM supplemented with 10% FBS. CHO cells stably expressing αIIbβ3 integrin were obtained from the laboratory of M. Chignard (Université François Rabelais, Tours, France; Si-Tahar et al., 1997). The CHO-αIIbβ3 cells were cultured in MEM supplemented with 10% FBS. Human lung adenocarcinoma H1299 cells were maintained in RPMI 1640 medium (Hyclone) with 10% FBS. All cells were maintained at 37°C and 5% CO_2 and passaged using 0.25% trypsin/0.02% EDTA for dissociation at ∼80% confluence. For plasmid transfections, cells were grown at 60∼80% confluence. Cells were transfected with Sage LipoPlus^T Transfection Reagent (Beijing Sage Creation Science) or polyethylenimine (Polyscience) according to the manufacturer's protocol.

Mouse tissue analysis

Smurf1 WT and KO mice were gifts from P. Wang (East China Normal University, Shanghai, China). In brief, WT and knockout littermates were killed, and tissues were frozen and resolved in RIPA buffer (50 mM Tris-HCl, 150 mM NaCl, pH 7.4, 0.5% sodium deoxycholate, 1% NP-40, and 0.1% SDS) supplemented with 1 mM $NaVO_3$, 1 mM NaF, 1 mM EGTA, 5 mM EDTA, and 1 mM DTT. The paired samples were subjected to immunoblotting with indicated antibodies. The experiments were approved by the Ethics Committee of Beijing Institute of Radiation Medicine.

Immunoprecipitation and immunoblotting

Cell lysates were prepared in RIPA buffer with protease inhibitor cocktail. For each immunoprecipitation assay, 2 mg protein was used, and 2 µg of indicated antibodies was added for each reaction. Isotype-matched IgG was used as a negative control. Antibodies were mixed with equal amounts of protein lysate and incubated at 4°C overnight with rotation. Lysates were incubated with 50 µl of 50% protein A or G agarose (Santa Cruz Biotechnology, Inc.) with rotation for 3 h. Then beads were washed with RIPA buffer three times. Immunoprecipitates were resolved by SDS-PAGE, transferred to PVDF membranes, and analyzed by immunoblotting. Transfer membranes were probed with indicated primary and secondary antibodies. The membranes were analyzed with the Super Signal chemiluminescence kit (Thermo Fisher Scientific). ImageJ was used for quantification analysis of the band density of target proteins. All of the immunoprecipitation and Western blots were repeated at least three times.

Protein expression and pull-down

To obtain the GST fusion proteins of Smurf1, the DNA fragment of Smurf1 was subcloned into pGEX-4T-1 vector (GE Healthcare). GST and GST-fusion proteins were expressed in *Escherichia coli* BL21 (Tiangen Biotech) and purified with glutathione-Sepharose 4B beads (Pharmacia Biotech). His-MBP-Kindlin-2 was expressed in *E. coli* BL21 and purified with His-Select HF Nickel Affinity Gel (Sigma-Aldrich). To detect the direct binding of Kindlin-2 with Smurf1, GST or GST-smurf1 was immobilized on GST 4B beads and washed, then beads were incubated with His-MBP-Kindlin-2 purified by MBP Affinity Matrix (Amylose Resin; New England Biolabs, Inc.) or His-Select HF Nickel Affinity Gel for 12 h at 4°C under rotation. Bacterial-expressed His-MBP-Kindlin-2 bound to MBP Affinity Matrix or His-Select HF Nickel Affinity Gel was incubated with GST-Smurf1 or GST for 12 h at 4°C. Then beads were washed with RIPA buffer three times, and proteins were eluted, followed by Western blot analysis.

RNA interference

A specific siRNA targeting human Kindlin-2 was designed according to the human Kindlin-2 cDNA sequence and synthesized by QIAGEN. The sense targeting sequence was as follows: 5′-AAGCUGGUGGAG AAACUCG-3′. Two siRNAs targeting human Smurf1 were designed and synthesized by RiboBio. Sense targeting sequences were as follows: (1) 5′-GGGCUCUUCCAGUAUUCUATT-3′; (2) 5′-GCAUCG AAGUGUCCAGAGAAG-3′; SiRNA sequences targeting mouse Smurf1: (1) 5′-CCAGTATTCCACGGACAAT-3′; (2) 5′-CCGACA CUGUGAAAAACACTT-3′; and (3) 5′-GCGUUUGGAUCUAUG CAAATT-3′. An irrelevant dsRNA with the sense sequence 5′-UUC UCCGAACGUGUCACGU-3′ was used as control. For siRNA transfections, cells were grown at ∼60% confluence and transfected with Lipofectamine RNAiMAX Transfection Reagent according to the manufacturer's protocol.

In vivo and in vitro ubiquitination assays

For in vivo ubiquitination assays, a 10-cm dish of HEK293T cells was used for each group. Cells were grown at ∼80% confluence and transiently transfected with 3 µg Flag-Kindlin-2 (or mutants), 4 µg HA-Ub (or mutants), and 4 µg Myc-Smurf1 WT or E3-inactive mutant (C699A) by polyethylenimine. After transfection for 24 h, cells were washed twice with cold PBS and lysed in RIPA lysis buffer for 30 min on ice. Cells were collected and centrifuged at ∼12,000 rpm for 15 min to pellet the cell debris. Cell lysates were incubated with 20 µl of 50% anti-Flag M2 beads (Sigma-Aldrich) for 3 h at 4°C. After extended washes, the immune complexes were analyzed using SDS-PAGE and transferred to membranes for detection of ubiquitination by anti-HA immunoblotting.

For in vitro ubiquitination assays, GST and GST-Smurf1 (WT or C699A mutant) and His-Kindlin-2 was expressed in Sf9 insect cells and purified by HisTrap HP (GE Healthcare) In vitro ubiquitination was performed in 30 µl ubiquitination reaction buffer with 0.7 µg E1, 1 µg UbcH5c (E2), 15 µg HA-ubiquitin (all from Boston Biochem), 0.7 µg His-Kindlin-2, and 1.5 µg GST or GST-Smurf1 (WT or C699A mutant), and the reaction mixture was incubated at 30°C for 2 h. Then GST 4B beads were added to the reaction mixture to avoid the contamination of the auto-ubiquitination of GST-Smurf1. Supernatant was separated and collected from insoluble material by centrifugation. The reaction was terminated with SDS sample buffer.

Immunofluorescence and confocal microscopy

The cells cultured on coverslips were washed with cold PBS twice, fixed in 4% PFA for 15 min, and permeabilized with 0.5% Triton X-100 for 10 min. To avoid nonspecific staining, cells were incubated with 5% BSA for 1 h at RT and stained with the indicated primary antibodies for 14 h at 4°C, followed by incubating with secondary antibodies conjugated with Alexa Fluor 488, 568, or 633 (Invitrogen) for 45 min at room temperature. Cells were also stained with DAPI to visualize the nuclei. The stained cells were visualized at 63× or 100× using an LSM 780 laser scanning confocal microscope (ZEISS), the image collecting software was Zen Black (ZEISS), and images were exported with Zen Blue (ZEISS). The excitation wavelengths were, for DAPI, 405 nm; for Alexa Fluor 488, 488 nm; for Alexa Fluor 568, 543 nm; and for Alexa Fluor 633, 621 nm. The image size was 1,024 × 1,024 pixels, and images were processed with ImageJ.

Integrin αIIbβ3 activation assay

Integrin αIIbβ3 activation assay was performed according to the method reported (Shi et al., 2007; Montanez et al., 2008). In brief, CHO cells expressing αIIbβ3 integrin were transfected with indicated plasmids. 48 h after transfection, the cells were harvested and suspended in HBSS buffer (1% BSA, 0.5 mM $CaCl_2$, and 0.5 mM $MgCl_2$) for 40 min at RT. Cells were washed twice and stained with a secondary anti-mouse IgM Alexa Fluor 647–labeled antibody (Invitrogen) for 30 min on ice. PAC-1 binding was measured with a FACSCalibur (BD). PAC1 binding was first normalized to αIIbβ3 expression level on the cell surface, which is measured by PAC1 binding of different groups of cells treated with Mn^{2+} (2 mM). The mean fluorescence intensity (MFI) index was calculated as (MFI of PAC-1 binding of each group)/(MFI of maximal PAC-1 binding in the cells treated with 2 mm Mn^{2+} of each group). Relative integrin activation was calculated as (MFI index of experimental group)/(MFI index of control group), and the integrin activation of the control group was defined as 1.0. To consider whether expression of various constructs in the αIIbβ3 CHO cells affected surface expression levels of the integrin, we evaluated reactivity with a mAb recognizing total integrin αIIbβ3, which reacts with αIIbβ3 independently of its activation state.

Integrin β1 activation assay

Integrin β1 activation was analyzed as described (Arjonen et al., 2012). In brief, cells were diluted in culture medium with 30 mM Hepes (pH 7.4). Cells were lifted on ice, and cell-surface β1 integrin was stained with 9EG7 (active integrin β1 antibody) or total integrin β1 antibody for 60 min at 4°C, followed by counterstaining with 1:400 diluted Alexa Fluor 488–conjugated secondary antibodies for 60 min at 4°C. Cells were analyzed using FACSCalibur. The integrin activation index is defined as the MFI of 9EG7 staining (active integrin β1) divided by the MFI of total integrin β1 staining.

Cell spreading and FA formation analyses

For cell spreading and focal adhesion analyses, cells were replated at a density of 1×10^5 cells per six-well dish on FN-, vitronectin-, or collagen-coated coverslips (5 µg/ml) over varying time periods and then photographed using light or confocal microscopy. For further examination of cell spreading and FA formation, cells were fixed after 15 min of plating in 4% PFA and stained for paxillin or Kindlin-2. For dynamic spreading assays, indicated siRNAs or plasmids were transfected into HeLa cells, and the cells were seeded onto 5 µg/ml FN–coated non-treated six-well plates and maintained at 37°C and 5% CO_2 on the microscope stage. Cells were visualized with Axiocam MRm (ZEISS), and images were collected with Zen Black software and processed with ImageJ. The objective lens was 20×, and cells were visualized for a total duration of 120 min. Flattened and well-spread cells at indicated times were counted.

For FA quantification, 10 different fields of cells were photographed for each group. The focal adhesions (stained with paxillin) of

each cell were visualized by paxillin localization and outlined by ImageJ, then quantified by manual point-counting, because thresholded objects were occasionally not separable, and some tiny spots were erroneously counted as FAs.

Analyses of FA dynamics

Cells expressing zyxin-EGFP were transfected with control siRNA or smurf1 siRNA for 48 h, then plated on a 5 µg/ml FN–coated glass-bottom dish for 2 h. Time lapse images were collected by a confocal microscope (LSM 780; ZEISS) with a custom-imaging chamber maintained at 37°C and pH 7.4 throughout the observation period. The cells were visualized at 100× using an LSM 780 laser scanning confocal microscope, and images were collected with Zen Black. Analysis of FA assembly and disassembly was performed as previously described (Webb et al., 2004). The FA lifespan was the length of time a FA was visible during the time of acquisition.

Cell adhesion assay

Nontreated six-well plates were coated with FN, vitronectin, or collagen (diluted in PBS) for 1 h at 37°C. Wells were blocked with 1% heat-denatured BSA for 1 h at 37°C. Cell suspensions (1 ml) were seeded into the wells in triplicate at 1×10^5 cells/well in cell adhesion buffer (RPMI 1640, 2 mM $CaCl_2$, 1 mM $MgCl_2$, 0.2 mM $MnCl_2$, and 0.5% BSA) and allowed to attach for indicated times at 37°C in an atmosphere with 5% CO_2. After three washes with PBS to remove nonbound cells, adherent cells were photographed and counted under a microscope (CKX41; Olympus) with a 10× objective; 10 randomly fields were selected in each well. Three independent experiments were run in triplicate.

Tissue samples and immunohistochemistry

Surgically removed colonic cancer tissues and adjacent normal tissues were collected from three patients at Peking University Third Hospital (Beijing, China) and used for Western blot analysis. The experiments were approved by the Ethics Committee of Peking University Third Hospital.

Immunohistochemical staining for specific protein expression was performed on mouse tissue sections. In brief, sections (4 mm thick) were deparaffinized with xylene, followed by rehydration in ethanol. Hydrogen peroxide (3%) was used to eliminate endogenous peroxidase. Sections were incubated overnight at 4°C with primary antibodies against Kindlin-2 (Sigma-Aldrich), 1:200; Smurf1 (Abcam), 1:100; and Smad1 (Bioss), 1:100. After extensive washing in PBS buffer, sections were incubated for 30 min with secondary antibodies (Dako). Immunostaining was examined with a BX51 microscope (Olympus), and images were photographed with a 40× objective.

Statistical analysis

Data are presented as mean ± SD. Comparisons between two groups were made using two-tailed Student's *t* test. Differences among more than two groups were compared using one-way ANOVA. Pairwise comparisons were evaluated by the Student–Newman–Keuls procedure or Dunnett's T3 procedure when the assumption of equal variances did not hold. $P < 0.05$ was considered statistically significant. Statistical analyses were conducted with SPSS 19.0.

Online supplemental material

Fig. S1 shows that Smurf1 inhibits integrin β1 activation in fibroblasts. Fig. S2 shows that Smurf1 promotes Kindlin-2 degradation in various cell lines. Fig. S3 demonstrates that Smurf1 does not have an effect on Talin-H degradation. Fig. S4 shows the function of Kindlin-2 PY motif mutant in integrin activation and cell spreading. Fig. S5 shows that Smurf1 suppresses cell spreading, adhesion, and FA formation. Table S1 shows the ubiquitination sites of Kindlin-2 identified by mass spectrometric analysis. Table S2 shows the ubiquitination sites of Talin-H identified by mass spectrometric analysis.

Acknowledgments

This work was supported by grants from the Chinese Ministry of Science and Technology (2016YFC1302103, 2015CB553906, and 2013CB910501), the National Natural Science Foundation of China (81230051, 81472734, and 31170711), Natural Science Foundation of Beijing Municipality (grants 7120002 and 7171005), the 111 Project of the Ministry of Education of China, Peking University (grants BMU20120314 and BMU20130364), and a Leading Academic Discipline Project of the Beijing Education Bureau to H. Zhang. This work was also supported by grants from the National Natural Science Foundation of China (81300563 and 81670626) and a Postdoctoral Fellowship from the Peking-Tsinghua Center for Life Sciences to X. Wei.

The authors declare no competing financial interests.

Author contributions: X. Wei designed the research, did experimental work, analyzed data, and wrote the manuscript. X. Wang designed the research, did experimental work, and analyzed data. J. Zhan and Y. Chen did experimental work. W. Fang participated in study design. L. Zhang participated in study design and revised the manuscript. H. Zhang designed and conceptualized the research, supervised the experimental work, and wrote the manuscript.

Submitted: 16 September 2016
Revised: 11 January 2017
Accepted: 2 March 2017

References

Al-Hakim, A.K., A. Zagorska, L. Chapman, M. Deak, M. Peggie, and D.R. Alessi. 2008. Control of AMPK-related kinases by USP9X and atypical Lys(29)/Lys(33)-linked polyubiquitin chains. *Biochem. J.* 411:249–260. http://dx.doi.org/10.1042/BJ20080067

An, Z., K. Dobra, J.G. Lock, S. Strömblad, A. Hjerpe, and H. Zhang. 2010. Kindlin-2 is expressed in malignant mesothelioma and is required for tumor cell adhesion and migration. *Int. J. Cancer.* 127:1999–2008. http://dx.doi.org/10.1002/ijc.25223

Arjonen, A., J. Alanko, S. Veltel, and J. Ivaska. 2012. Distinct recycling of active and inactive β1 integrins. *Traffic.* 13:610–625. http://dx.doi.org/10.1111/j.1600-0854.2012.01327.x

Byron, A., J.D. Humphries, J.A. Askari, S.E. Craig, A.P. Mould, and M.J. Humphries. 2009. Anti-integrin monoclonal antibodies. *J. Cell Sci.* 122:4009–4011. http://dx.doi.org/10.1242/jcs.056770

Calderwood, D.A., R. Zent, R. Grant, D.J. Rees, R.O. Hynes, and M.H. Ginsberg. 1999. The Talin head domain binds to integrin β subunit cytoplasmic tails and regulates integrin activation. *J. Biol. Chem.* 274:28071–28074. http://dx.doi.org/10.1074/jbc.274.40.28071

Cao, Y., and L. Zhang. 2013. A Smurf1 tale: Function and regulation of an ubiquitin ligase in multiple cellular networks. *Cell. Mol. Life Sci.* 70:2305–2317. http://dx.doi.org/10.1007/s00018-012-1170-7

Chong, P.A., H. Lin, J.L. Wrana, and J.D. Forman-Kay. 2010. Coupling of tandem Smad ubiquitination regulatory factor (Smurf) WW domains modulates target specificity. *Proc. Natl. Acad. Sci. USA.* 107:18404–18409. http://dx.doi.org/10.1073/pnas.1003023107

David, D., S.A. Nair, and M.R. Pillai. 2013. Smurf E3 ubiquitin ligases at the cross roads of oncogenesis and tumor suppression. *Biochim. Biophys. Acta.* 1835:119–128.

Desgrosellier, J.S., and D.A. Cheresh. 2010. Integrins in cancer: Biological implications and therapeutic opportunities. *Nat. Rev. Cancer.* 10:9–22. http://dx.doi.org/10.1038/nrc2748

Horiki, M., T. Imamura, M. Okamoto, M. Hayashi, J. Murai, A. Myoui, T. Ochi, K. Miyazono, H. Yoshikawa, and N. Tsumaki. 2004. Smad6/Smurf1 overexpression in cartilage delays chondrocyte hypertrophy and causes

dwarfism with osteopenia. *J. Cell Biol.* 165:433–445. http://dx.doi.org/10.1083/jcb.200311015

Huang, C. 2010. Roles of E3 ubiquitin ligases in cell adhesion and migration. *Cell Adhes. Migr.* 4:10–18. http://dx.doi.org/10.4161/cam.4.1.9834

Huang, C., Z. Rajfur, N. Yousefi, Z. Chen, K. Jacobson, and M.H. Ginsberg. 2009. Talin phosphorylation by Cdk5 regulates Smurf1-mediated Talin head ubiquitylation and cell migration. *Nat. Cell Biol.* 11:624–630. http://dx.doi.org/10.1038/ncb1868

Huang, H., M.S. Jeon, L. Liao, C. Yang, C. Elly, J.R. Yates III, and Y.C. Liu. 2010. K33-linked polyubiquitination of T cell receptor-zeta regulates proteolysis-independent T cell signaling. *Immunity.* 33:60–70. http://dx.doi.org/10.1016/j.immuni.2010.07.002

Hynes, R.O. 2002. Integrins: Bidirectional, allosteric signaling machines. *Cell.* 110:673–687. http://dx.doi.org/10.1016/S0092-8674(02)00971-6

Ikeda, F., and I. Dikic. 2008. Atypical ubiquitin chains: New molecular signals. 'Protein Modifications: Beyond the Usual Suspects' review series. *EMBO Rep.* 9:536–542. http://dx.doi.org/10.1038/embor.2008.93

Inoue, Y., and T. Imamura. 2008. Regulation of TGF-β family signaling by E3 ubiquitin ligases. *Cancer Sci.* 99:2107–2112. http://dx.doi.org/10.1111/j.1349-7006.2008.00925.x

Kim, C., F. Ye, and M.H. Ginsberg. 2011. Regulation of integrin activation. *Annu. Rev. Cell Dev. Biol.* 27:321–345. http://dx.doi.org/10.1146/annurev-cellbio-100109-104104

Kulathu, Y., and D. Komander. 2012. Atypical ubiquitylation—The unexplored world of polyubiquitin beyond Lys48 and Lys63 linkages. *Nat. Rev. Mol. Cell Biol.* 13:508–523. http://dx.doi.org/10.1038/nrm3394

Lai-Cheong, J.E., M. Parsons, and J.A. McGrath. 2010. The role of kindlins in cell biology and relevance to human disease. *Int. J. Biochem. Cell Biol.* 42:595–603. http://dx.doi.org/10.1016/j.biocel.2009.10.015

Larjava, H., E.F. Plow, and C. Wu. 2008. Kindlins: Essential regulators of integrin signalling and cell-matrix adhesion. *EMBO Rep.* 9:1203–1208. http://dx.doi.org/10.1038/embor.2008.202

Legate, K.R., S.A. Wickström, and R. Fässler. 2009. Genetic and cell biological analysis of integrin outside-in signaling. *Genes Dev.* 23:397–418. http://dx.doi.org/10.1101/gad.1758709

Lu, K., X. Yin, T. Weng, S. Xi, L. Li, G. Xing, X. Cheng, X. Yang, L. Zhang, and F. He. 2008. Targeting WW domains linker of HECT-type ubiquitin ligase Smurf1 for activation by CKIP-1. *Nat. Cell Biol.* 10:994–1002. http://dx.doi.org/10.1038/ncb1760

Ma, Y.Q., J. Yang, M.M. Pesho, O. Vinogradova, J. Qin, and E.F. Plow. 2006. Regulation of integrin αIIbβ3 activation by distinct regions of its cytoplasmic tails. *Biochemistry.* 45:6656–6662. http://dx.doi.org/10.1021/bi060279h

Ma, Y.Q., J. Qin, C. Wu, and E.F. Plow. 2008. Kindlin-2 (Mig-2): A co-activator of β3 integrins. *J. Cell Biol.* 181:439–446. http://dx.doi.org/10.1083/jcb.200710196

Margadant, C., and A. Sonnenberg. 2010. Integrin-TGF-β crosstalk in fibrosis, cancer and wound healing. *EMBO Rep.* 11:97–105. http://dx.doi.org/10.1038/embor.2009.276

Meves, A., C. Stremmel, K. Gottschalk, and R. Fässler. 2009. The Kindlin protein family: New members to the club of focal adhesion proteins. *Trends Cell Biol.* 19:504–513. http://dx.doi.org/10.1016/j.tcb.2009.07.006

Montanez, E., S. Ussar, M. Schifferer, M. Bösl, R. Zent, M. Moser, and R. Fässler. 2008. Kindlin-2 controls bidirectional signaling of integrins. *Genes Dev.* 22:1325–1330. http://dx.doi.org/10.1101/gad.469408

Nie, J., L. Liu, G. Xing, M. Zhang, R. Wei, M. Guo, X. Li, P. Xie, L. Li, F. He, et al. 2014. CKIP-1 acts as a colonic tumor suppressor by repressing oncogenic Smurf1 synthesis and promoting Smurf1 autodegradation. *Oncogene.* 33:3677–3687. http://dx.doi.org/10.1038/onc.2013.340

Pickart, C.M. 2001. Mechanisms underlying ubiquitination. *Annu. Rev. Biochem.* 70:503–533. http://dx.doi.org/10.1146/annurev.biochem.70.1.503

Plow, E.F., J. Qin, and T. Byzova. 2009. Kindling the flame of integrin activation and function with kindlins. *Curr. Opin. Hematol.* 16:323–328. http://dx.doi.org/10.1097/MOH.0b013e32832ea389

Ren, Y., H. Jin, Z. Xue, Q. Xu, S. Wang, G. Zhao, J. Huang, and H. Huang. 2015. Kindlin-2 inhibited the growth and migration of colorectal cancer cells. *Tumour Biol.* 36:4107–4114. http://dx.doi.org/10.1007/s13277-015-3044-8

Sánchez, N.S., and J.V. Barnett. 2012. TGFβ and BMP-2 regulate epicardial cell invasion via TGFβR3 activation of the Par6/Smurf1/RhoA pathway. *Cell. Signal.* 24:539–548. http://dx.doi.org/10.1016/j.cellsig.2011.10.006

Shi, X., Y.Q. Ma, Y. Tu, K. Chen, S. Wu, K. Fukuda, J. Qin, E.F. Plow, and C. Wu. 2007. The MIG-2/integrin interaction strengthens cell-matrix adhesion and modulates cell motility. *J. Biol. Chem.* 282:20455–20466. http://dx.doi.org/10.1074/jbc.M611680200

Si-Tahar, M., D. Pidard, V. Balloy, M. Moniatte, N. Kieffer, A. Van Dorsselaer, and M. Chignard. 1997. Human neutrophil elastase proteolytically activates the platelet integrin αIIbβ3 through cleavage of the carboxyl terminus of the αIIb subunit heavy chain. Involvement in the potentiation of platelet aggregation. *J. Biol. Chem.* 272:11636–11647. http://dx.doi.org/10.1074/jbc.272.17.11636

Wang, H.R., Y. Zhang, B. Ozdamar, A.A. Ogunjimi, E. Alexandrova, G.H. Thomsen, and J.L. Wrana. 2003. Regulation of cell polarity and protrusion formation by targeting RhoA for degradation. *Science.* 302:1775–1779. http://dx.doi.org/10.1126/science.1090772

Webb, D.J., K. Donais, L.A. Whitmore, S.M. Thomas, C.E. Turner, J.T. Parsons, and A.F. Horwitz. 2004. FAK-Src signalling through paxillin, ERK and MLCK regulates adhesion disassembly. *Nat. Cell Biol.* 6:154–161. http://dx.doi.org/10.1038/ncb1094

Wei, X., Y. Xia, F. Li, Y. Tang, J. Nie, Y. Liu, Z. Zhou, H. Zhang, and F.F. Hou. 2013. Kindlin-2 mediates activation of TGF-β/Smad signaling and renal fibrosis. *J. Am. Soc. Nephrol.* 24:1387–1398. http://dx.doi.org/10.1681/ASN.2012101041

Wei, X., X. Wang, Y. Xia, Y. Tang, F. Li, W. Fang, and H. Zhang. 2014. Kindlin-2 regulates renal tubular cell plasticity by activation of Ras and its downstream signaling. *Am. J. Physiol. Renal Physiol.* 306:F271–F278. http://dx.doi.org/10.1152/ajprenal.00499.2013

Wu, C., H. Jiao, Y. Lai, W. Zheng, K. Chen, H. Qu, W. Deng, P. Song, K. Zhu, H. Cao, et al. 2015. Kindlin-2 controls TGF-β signalling and Sox9 expression to regulate chondrogenesis. *Nat. Commun.* 6:7531. http://dx.doi.org/10.1038/ncomms8531

Yamaguchi, K., O. Ohara, A. Ando, and T. Nagase. 2008. Smurf1 directly targets hPEM-2, a GEF for Cdc42, via a novel combination of protein interaction modules in the ubiquitin-proteasome pathway. *Biol. Chem.* 389:405–413. http://dx.doi.org/10.1515/BC.2008.036

Yamashita, M., S.X. Ying, G.M. Zhang, C. Li, S.Y. Cheng, C.X. Deng, and Y.E. Zhang. 2005. Ubiquitin ligase Smurf1 controls osteoblast activity and bone homeostasis by targeting MEKK2 for degradation. *Cell.* 121:101–113. http://dx.doi.org/10.1016/j.cell.2005.01.035

Ye, F., and B.G. Petrich. 2011. Kindlin: helper, co-activator, or booster of Talin in integrin activation? *Curr. Opin. Hematol.* 18:356–360. http://dx.doi.org/10.1097/MOH.0b013e3283497f09

Ye, F., A.K. Snider, and M.H. Ginsberg. 2014. Talin and kindlin: The one-two punch in integrin activation. *Front. Med.* 8:6–16. http://dx.doi.org/10.1007/s11684-014-0317-3

Yu, Y., J. Wu, L. Guan, L. Qi, Y. Tang, B. Ma, J. Zhan, Y. Wang, W. Fang, and H. Zhang. 2013. Kindlin 2 promotes breast cancer invasion via epigenetic silencing of the microRNA200 gene family. *Int. J. Cancer.* 133:1368–1379. http://dx.doi.org/10.1002/ijc.28151

Zhang, Y., H.R. Wang, and J.L. Wrana. 2004. Smurf1: A link between cell polarity and ubiquitination. *Cell Cycle.* 3:391–392. http://dx.doi.org/10.4161/cc.3.4.771

Zhu, H., P. Kavsak, S. Abdollah, J.L. Wrana, and G.H. Thomsen. 1999. A SMAD ubiquitin ligase targets the BMP pathway and affects embryonic pattern formation. *Nature.* 400:687–693. http://dx.doi.org/10.1038/23293